

VILA DO CONDE,
PORTUGAL,
29-31 MARCH, 2016

11th Iberian Cosmology Meeting

IBERICOS 2016

SOC ANA ACHÚCARRO (LEIDEN/BILBAO),
FERNANDO ATRIO-BARANDELA (SALAMANCA),
MAR BASTERO-GIL (GRANADA), JUAN GARCIA-
BELLIDO (MADRID), RUTH LAZKOZ (BILBAO),
CARLOS MARTINS (PORTO), JOSÉ PEDRO
MIMOSO (LISBON), DAVID MOTA (OSLO)

LOC ANA CATARINA LEITE, CARLOS MARTINS
(CHAIR), FERNANDO MOUCHEREK, PAULO
PEIXOTO (SYSADMIN), ANA MARTA PINHO,
IVAN RYBAK, ELSA SILVA (ADMIN)

SERIES OF MEETINGS WHICH AIM
TO ENCOURAGE INTERACTIONS
AND COLLABORATIONS BETWEEN
RESEARCHERS WORKING IN
COSMOLOGY AND RELATED
AREAS IN PORTUGAL AND SPAIN.

www.iastro.pt/ibericos2016





On the void explanation of the Cold Spot

Enrique Martínez-González

In coll. with Airam Marcos-Caballero, Raúl Fernández-Cobos and Patricio Vielva

Instituto de Física de Cantabria (CSIC-UC)

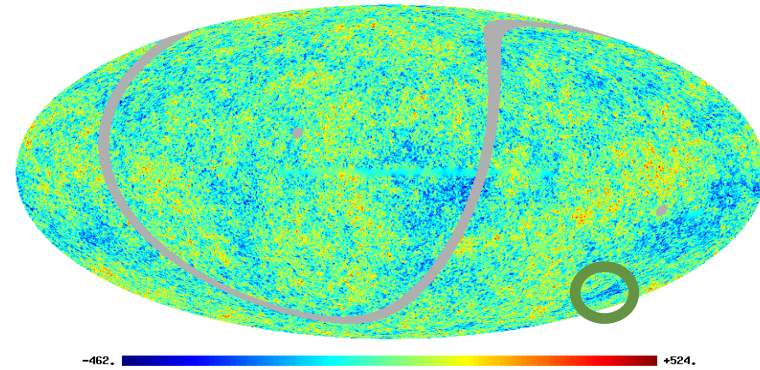
Summary

1. The Cold Spot CMB anomaly
2. Proposed interpretations
3. The void explanation
4. Considering extreme cases of voids
5. Conclusions

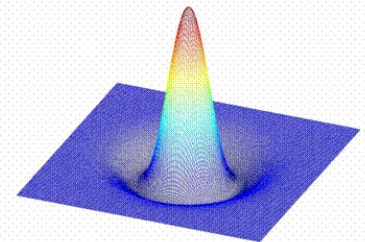
The Cold Spot CMB anomaly

- The Cold Spot anomaly was detected in the first year WMAP data by Vielva et al. 2004 by studying the moments of the Spherical Mexican Hat Wavelet coefficients.
- It was confirmed by Cruz et al. 2005 looking at the area of spots: The Cold Spot showed an anomalously large and cold area.
- It has a roundish shape and in terms of the SMHW coefficient at $R=5\text{deg}$ it represents a 4.7σ .
- Many other works have later confirmed its anomalous nature:
 - Foreground residuals or instrumental systematics have been excluded (Cruz et al. 2006)
 - Looking at different data sets, WMAP three (Cruz et al. 2007), five, seven and nine years data and Planck first year (Planck collaboration 2013. XXIII) and full data (Planck collaboration 2015. XVI).
 - Using other statistics: high order criticism (Cayón et al. 2005), directional wavelets (McEwen et al. 2005), scaling indices (Rath et al. 2007), needlets (Pietrobon et al. 2008), the Kolmogorov stochasticity parameter (Gurzadyan et al. 2009), temperature profile (Planck 2015).

Hemispherical asymmetry and cold spot



Spherical Mexican Hat Wavelet

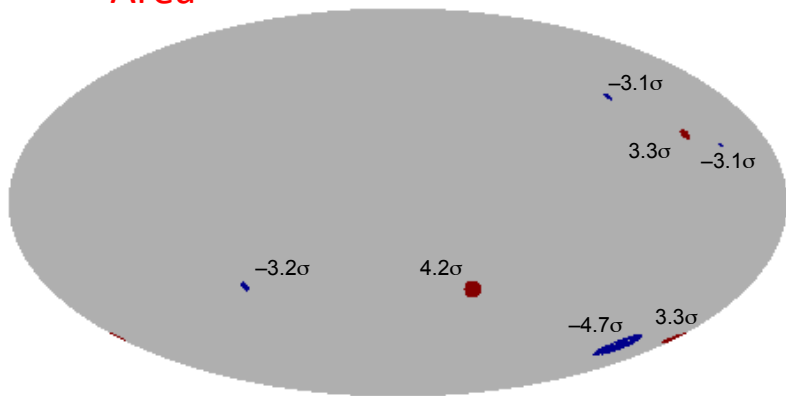


The Cold Spot CMB anomaly

Planck 2015 results. XVI. Isotropy and statistics of the CMB

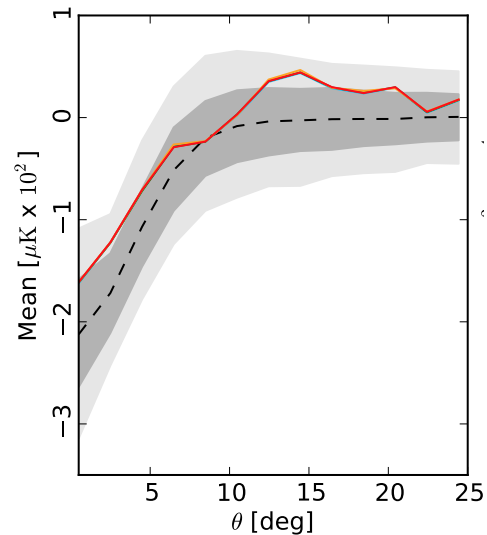
Area

$R = 300$ arcmin



Area	Scale [arcmin]	Probability [%]			
		Comm.	NILC	SEVEM	SMICA
SMHW					
Cold	200	3.8	5.1	3.7	3.8
	250	1.4	2.4	1.4	1.4
	300	0.4	1.5	0.4	0.4
	400	0.9	0.9	0.9	0.9
Hot	200	2.0	2.6	1.7	1.5
	250	2.4	3.0	2.1	2.0
	300	4.2	5.0	4.1	3.9
	400

Profile

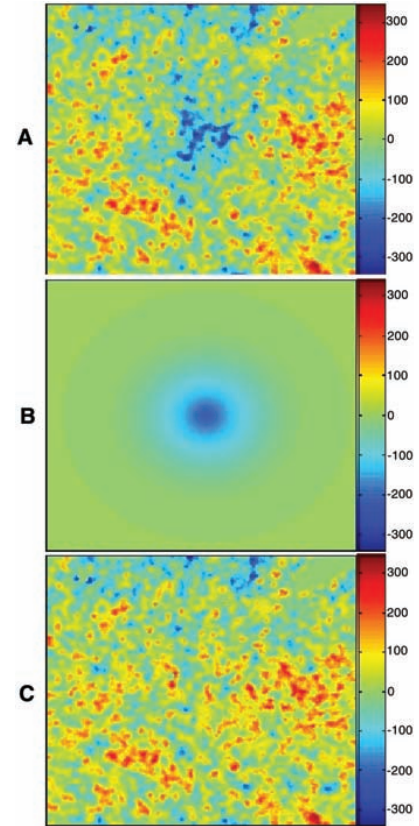


Angular profiles	Probability [%]			
	Comm.	NILC	SEVEM	SMICA
Mean	0.9	0.8	1.0	0.9

Proposed interpretations

- Statistical fluke at around 1% probability.
- Texture hypothesis (Cruz et al. 2007, Feeney et al. 2012)
- Bubble collision (Czech et al. 2010, McEwen et al. 2012, Feeney et al. 2013)
- Alternative inflationary models (Bueno Sánchez 2014)
- Void hypothesis (Tomita 2005, Inoue and Silk 2006, Rudnick et al. 2007, Cruz et al. 2008, Bremer et al. 2010, Granett et al. 2010)
- SZ effect, including the Eridanus cluster of galaxies (Cruz et al. 2008)
- **Non of the hypotheses have been either confirmed or discarded, except for the SZ effect.**

Texture hypothesis



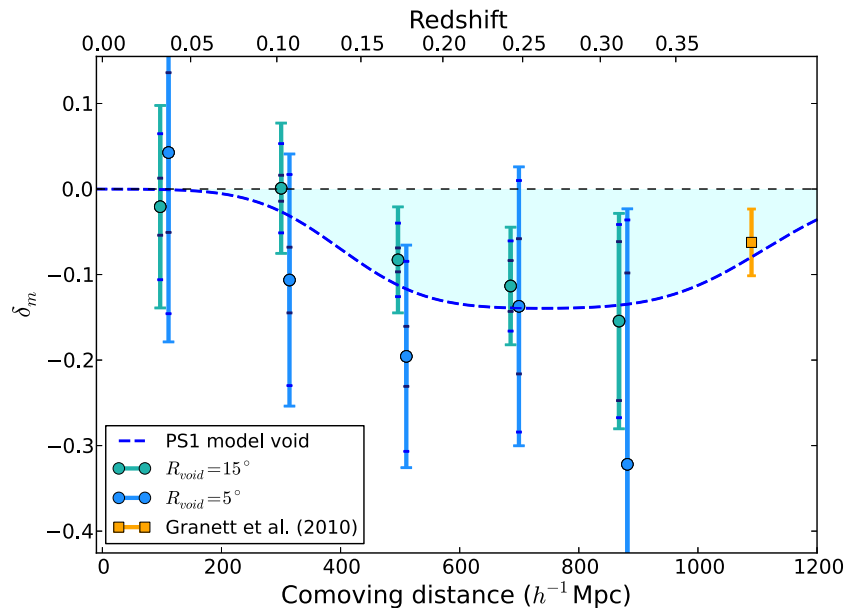
Void hypothesis

- The void origin has been recently invoked based on a super void found by Szapudi et al. (2015) in the WISE-2MASS-Pan-STARRS1 galaxy catalogue and independently by Finelli et al. (2016) in WISE-2MASS.

- Top-hat best-fitting parameters:

- $z_{\text{void}}=0.22\pm 0.03$
- $R_{\text{void}}=220\pm 50 h^{-1}\text{Mpc}$
- $\delta_m=-0.14\pm 0.04$

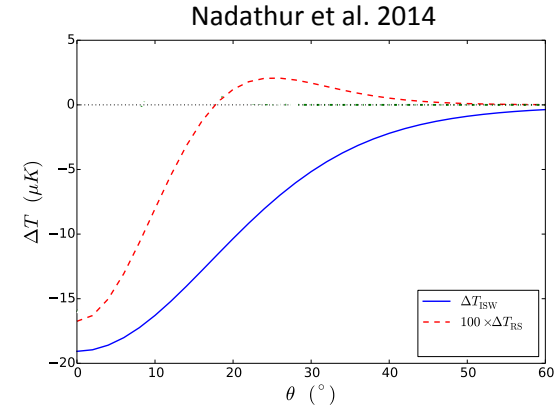
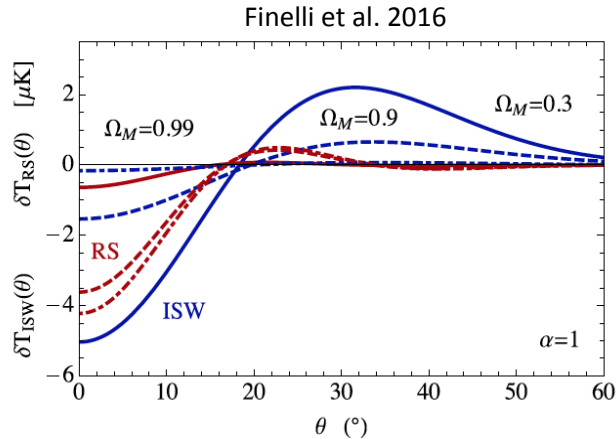
- This supervoid represents a 6σ fluctuation in the standard ΛCDM scenario.



ISW-RS profiles

- The non-linear Rees-Sciama effect in the LTB model has found to be negligible compared to the linear ISW one (Zibin 2014, Nadathur et al. 2014):

$$\Phi_0(r) \equiv \Phi_0 \exp \left[-\frac{r^2}{r_0^2} \right]$$



- The ISW effect can have a positive ring for specific profiles of the potential (Finelli et al. 2016):

$$\Phi_0(r) = \Phi_0 \left(1 - \alpha \frac{r^2}{r_0^2} \right) \exp \left[-\frac{r^2}{r_0^2} \right]$$

- N-body simulations also show a negligible RS effect compared to the linear ISW one (Cai et al. 2010).

Void explanation

- Marcos-Caballero, Fernández-Cobos, M-G and Vielva 2016 have reviewed the ISW contribution induced on the CMB by the Szapudi et al. 2015 supervoid. For a spherical model the ISW is given by:

$$\frac{\Delta T(\theta)}{T_{\text{CMB}}} = -2 \int dz \frac{dG(z)}{dz} \Phi \left(\sqrt{\chi^2(z) + \chi_0^2 - 2\chi(z)\chi_0 \cos \theta} \right)$$

- Two different density profiles are considered:
 - The top hat model (Szapudi et al. 2015):

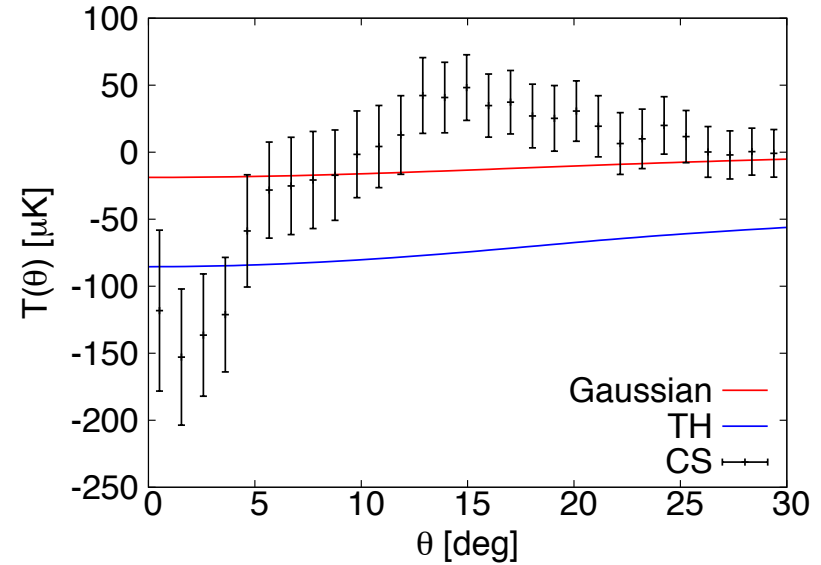
$$\Phi(r) = \begin{cases} \phi_0 R^2 \left(3 - \frac{r^2}{R^2} \right), & \text{if } r \leq R \\ \phi_0 \frac{2R^3}{r}, & \text{if } r > R, \end{cases}$$

- The Gaussian model (Finelli et al. 2016, Nadathur et al. 2014)

$$\Phi(r) = \phi_0 r_0^2 \exp \left(-\frac{r^2}{r_0^2} \right)$$

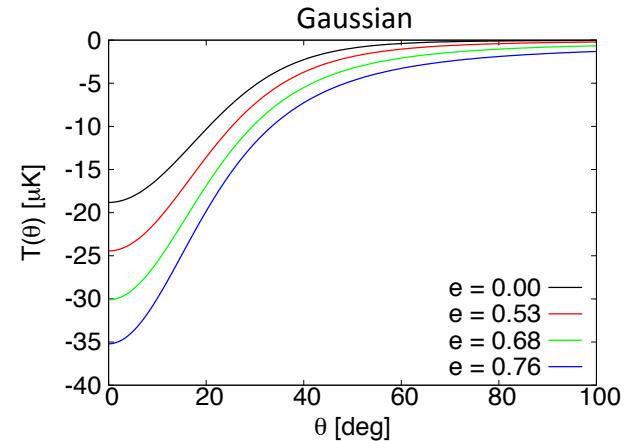
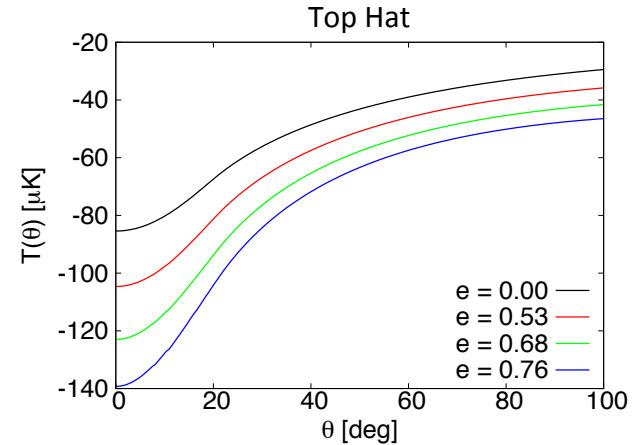
Spherical model

- Both the TH and the Gaussian void have amplitudes smaller than the CS and a much flatter profile.
- A quantity that takes into account both the amplitude and shape of the CS is the SMHW coefficient:
 - the CS is $-19.3 \mu\text{K}$, whereas the TH model produces $-1.07 \mu\text{K}$ and the Gaussian $-0.54 \mu\text{K}$.
 - The SMHW coefficient of the CS is 20 times larger than the typical ISW effect fluctuation ($\sigma_{\text{ISW}}=0.94 \mu\text{K}$).
- The CS is a 4.7σ fluctuation that after subtracting the void effect is still a $\approx 4.5\sigma$ fluctuation.



Elliptical model

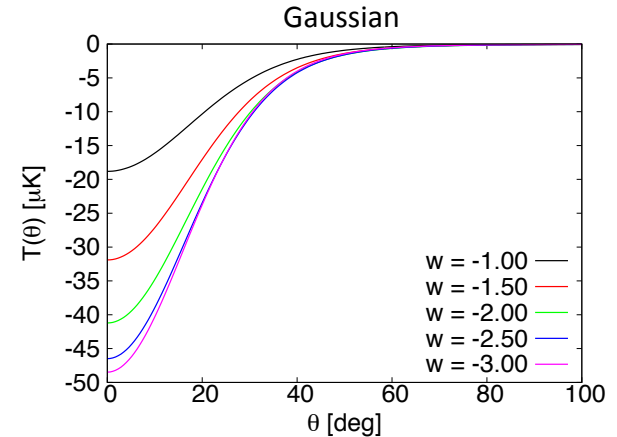
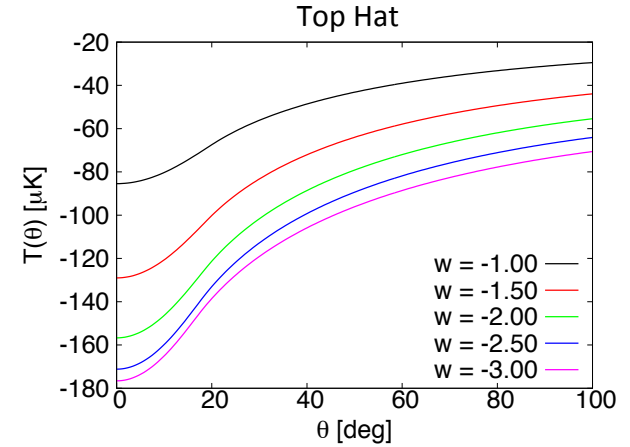
SMHW coefficient		
e	TH [μK]	Gaussian [μK]
0.00	-1.07	-0.54
0.53	-1.42	-0.71
0.68	-1.81	-0.85
0.76	-2.20	-1.03



The ISW profiles for the elliptical model differs from that of the CS.

Varying the DE equation of state parameter w

SMHW coefficient		
ω	TH [μK]	Gaussian [μK]
-1.00	-1.07	-0.54
-1.50	-1.74	-0.96
-2.00	-2.13	-1.28
-2.50	-2.34	-1.49
-3.00	-2.38	-1.60



The ISW profiles for different w values differ from that of the CS.

Conclusions and discussion

- The ISW effect from the supervoid recently discovered by Szapudi et al. 2015 does not account for the observed CS CMB decrement considering both its amplitude and shape.
- Even considering extreme scenarios in terms of the void ellipticity or the DE equation of state parameter, the SMHW coefficient is too small compared to the CS one.
- N-body simulations provide a ISW map consistent with Gaussian realisations (Cai et al. 2010, Watson et al. 2014).
- A situation with many aligned voids does not provide a satisfactory solution to explain the CS profile (Naidoo et al. 2015).
- The probability of finding such a supervoid in the direction of the CS and up to the explored redshift ($z \approx 1$) is of a few percent.
- **In conclusion, the ISW effect within the standard model is not a plausible explanation for the CS, not even considering the Rees-Sciama effect.**

VILA DO CONDE,
PORTUGAL,
29-31 MARCH, 2016

11th Iberian Cosmology Meeting

IBERICOS 2016

SOC ANA ACHÚCARRO (LEIDEN/BILBAO),
FERNANDO ATRIO-BARANDELA (SALAMANCA),
MAR BASTERO-GIL (GRANADA), JUAN GARCIA-
-BELLIDO (MADRID), RUTH LAZKOZ (BILBAO),
CARLOS MARTINS (PORTO), JOSÉ PEDRO
MIMOSO (LISBON), DAVID MOTA (OSLO)

LOC ANA CATARINA LEITE, CARLOS MARTINS
(CHAIR), FERNANDO MOUCHEREK, PAULO
PEIXOTO (SYSADMIN), ANA MARTA PINHO,
IVAN RYBAK, ELSA SILVA (ADMIN)

SERIES OF MEETINGS WHICH AIM
TO ENCOURAGE INTERACTIONS
AND COLLABORATIONS BETWEEN
RESEARCHERS WORKING IN
COSMOLOGY AND RELATED
AREAS IN PORTUGAL AND SPAIN.

www.iastro.pt/ibericos2016



Cold imprint of supervoids in the Cosmic Microwave Background

Andras Kovacs

Severo Ochoa Fellow, IFAE Barcelona



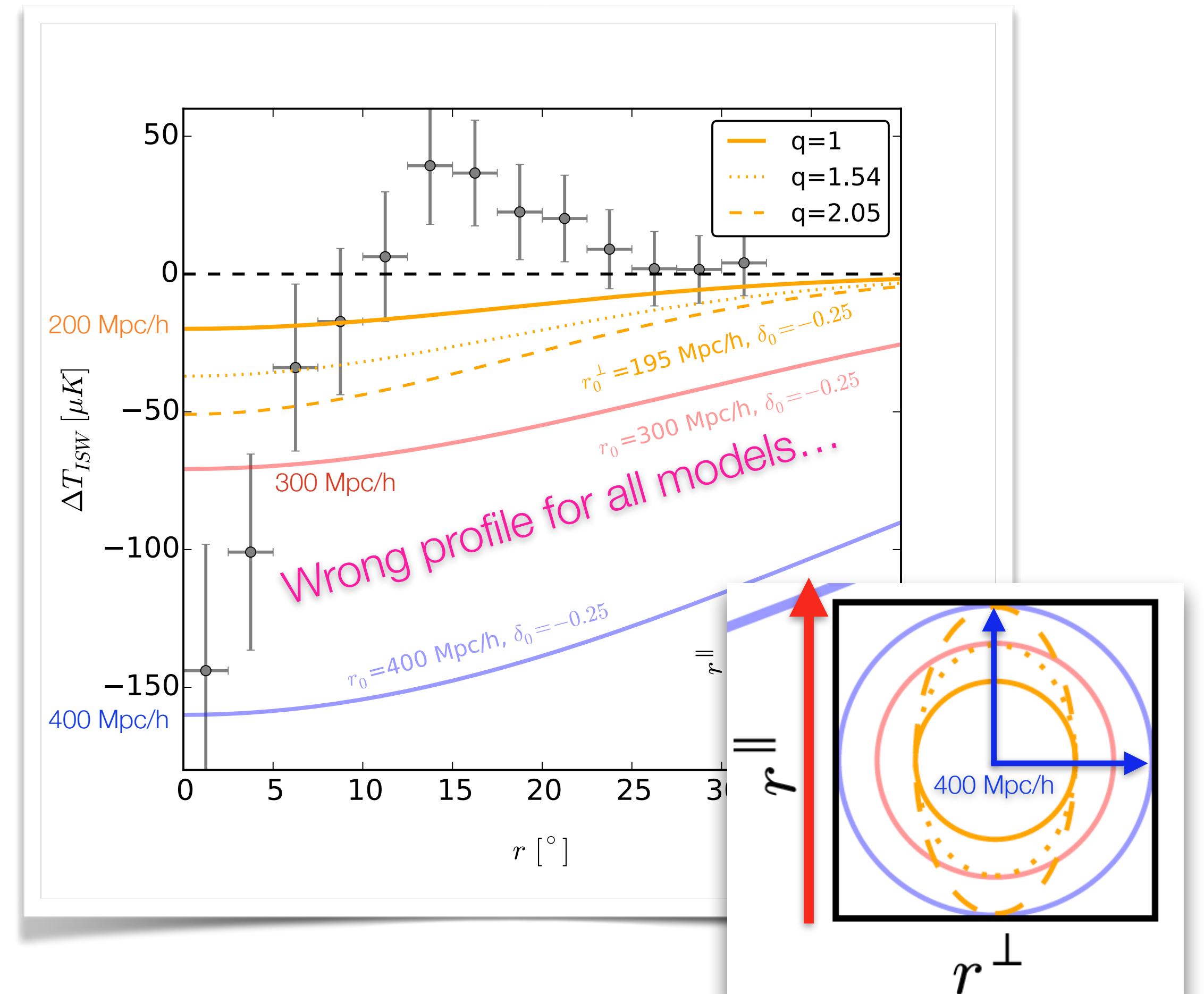
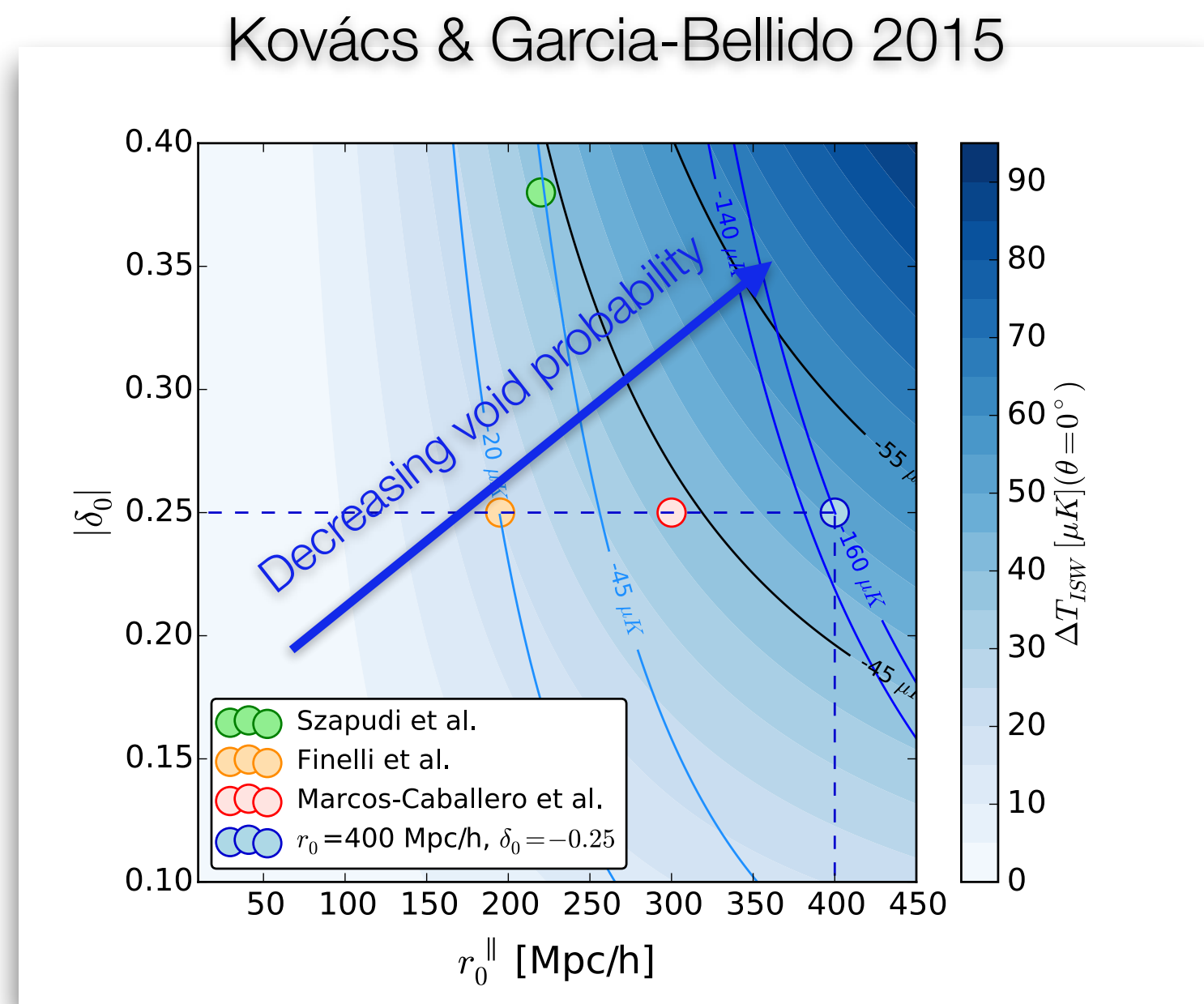
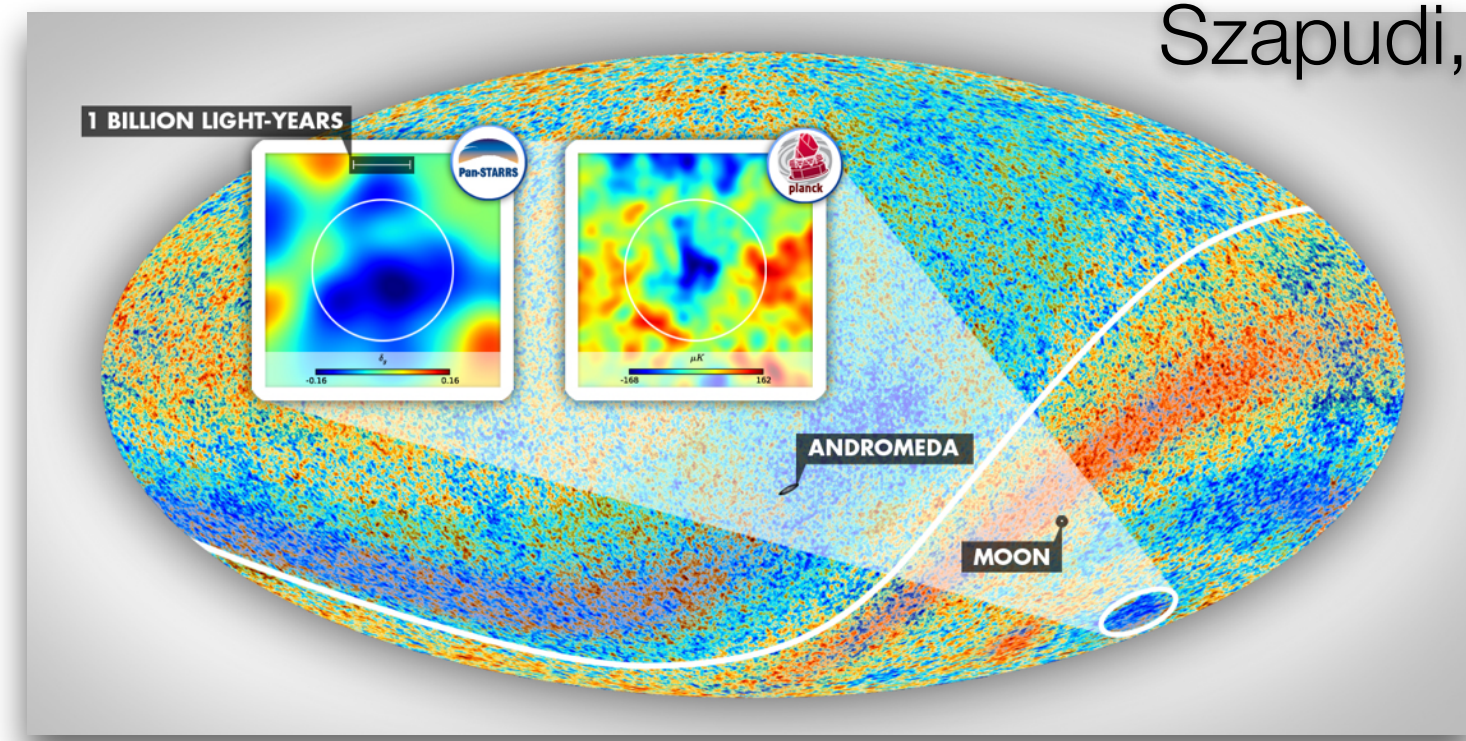
Barcelona Institute of
Science and Technology



EXCELENCIA
SEVERO
OCHOA

OCHOA

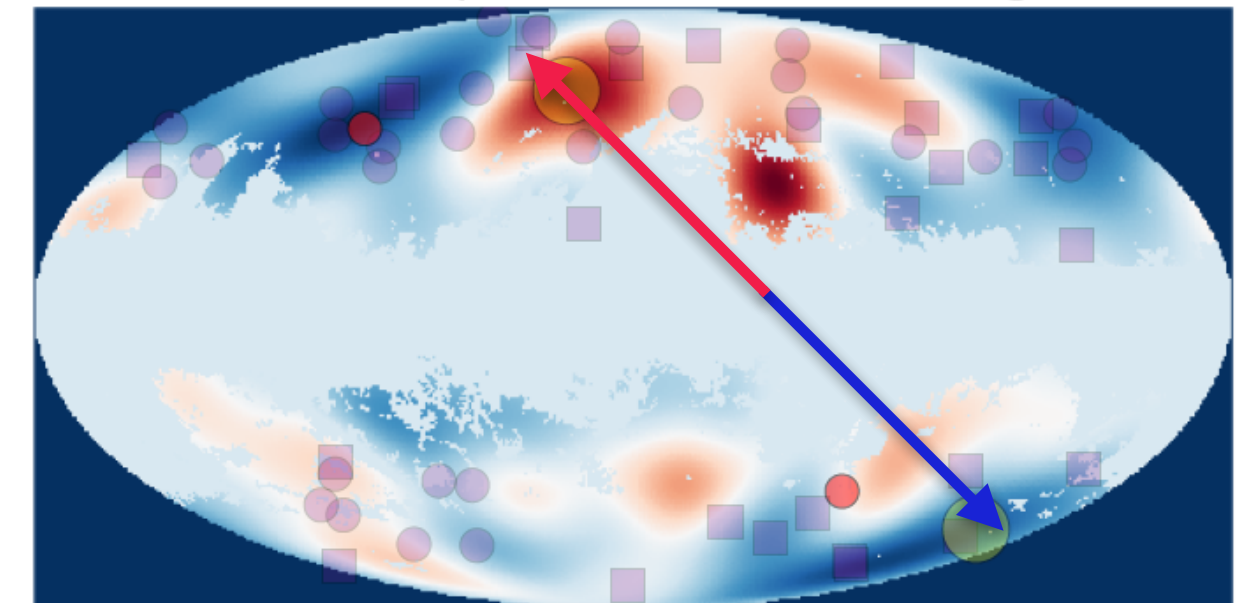
The Eridanus supervoid and the Cold Spot - **ISW?**



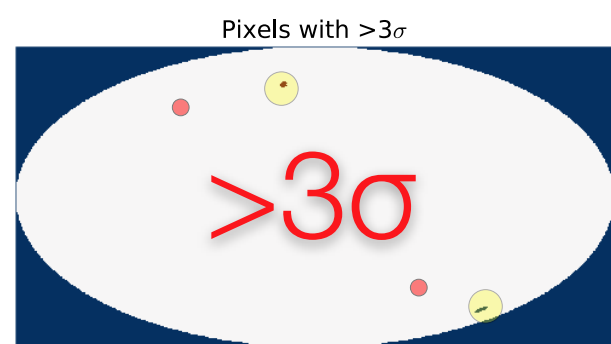
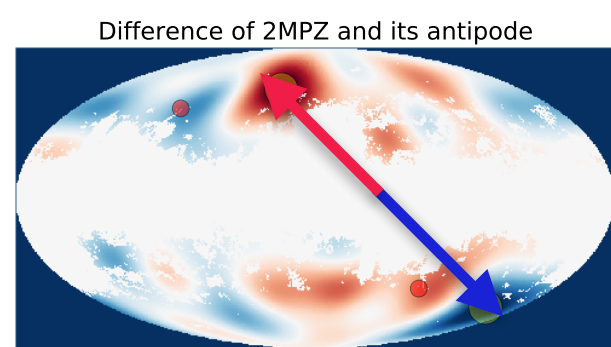
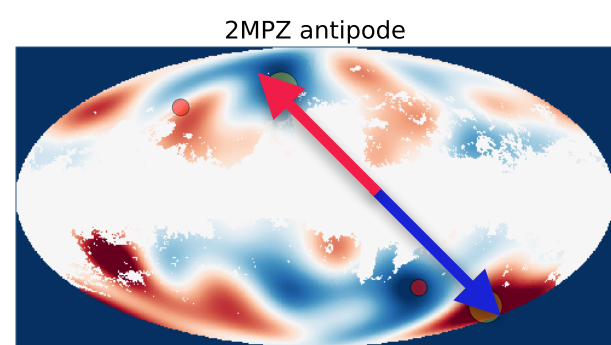
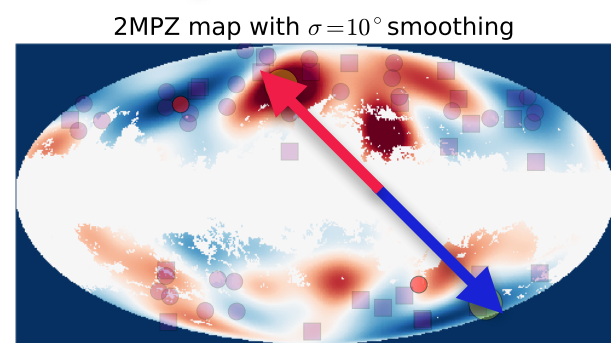
The 2MPZ survey of the Eridanus supervoid

Kovács & Garcia-Bellido 2015

2MPZ map with $\sigma=10^\circ$ smoothing

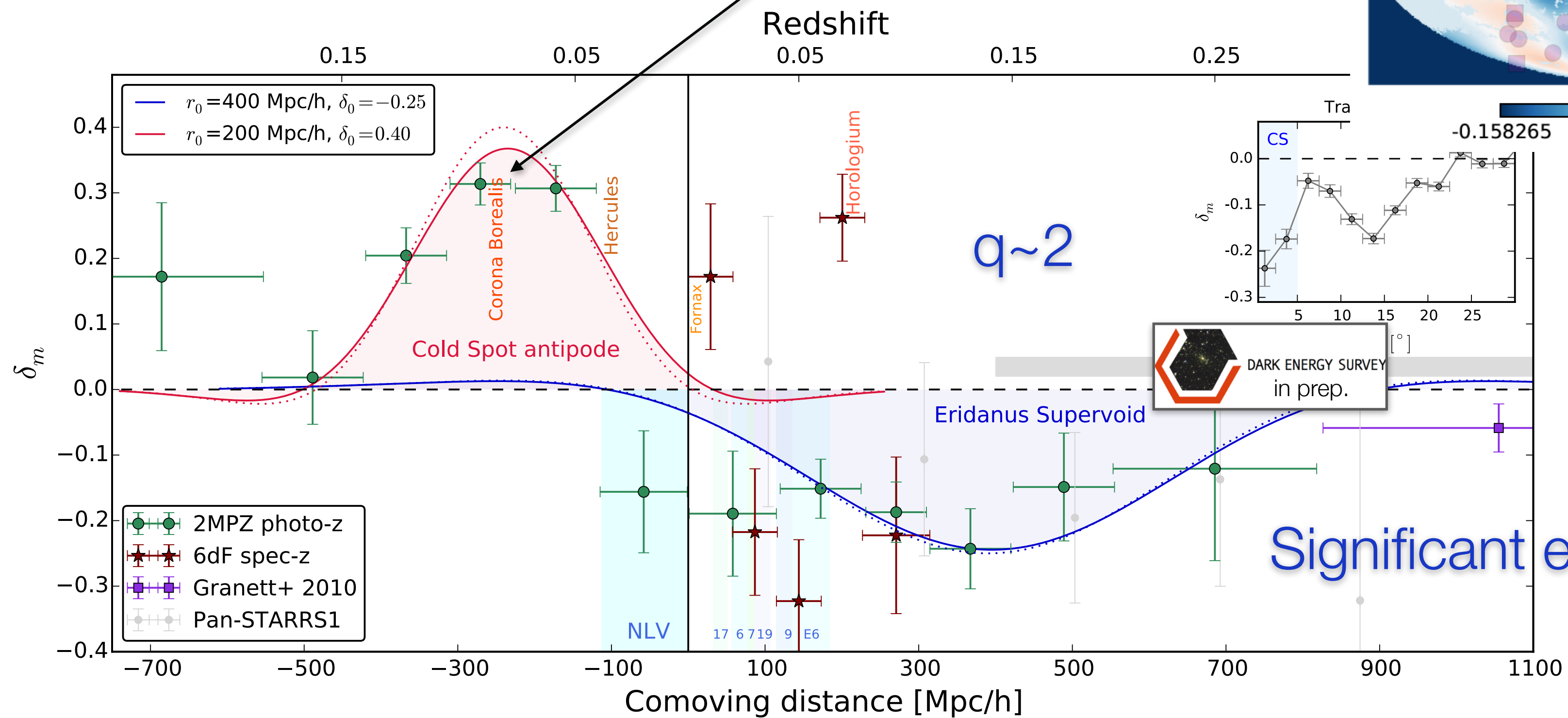


Antipode stat:



-3.01888 3.01888

SDSS Great Wall in the antipode



Significant elongation!

Its antipode

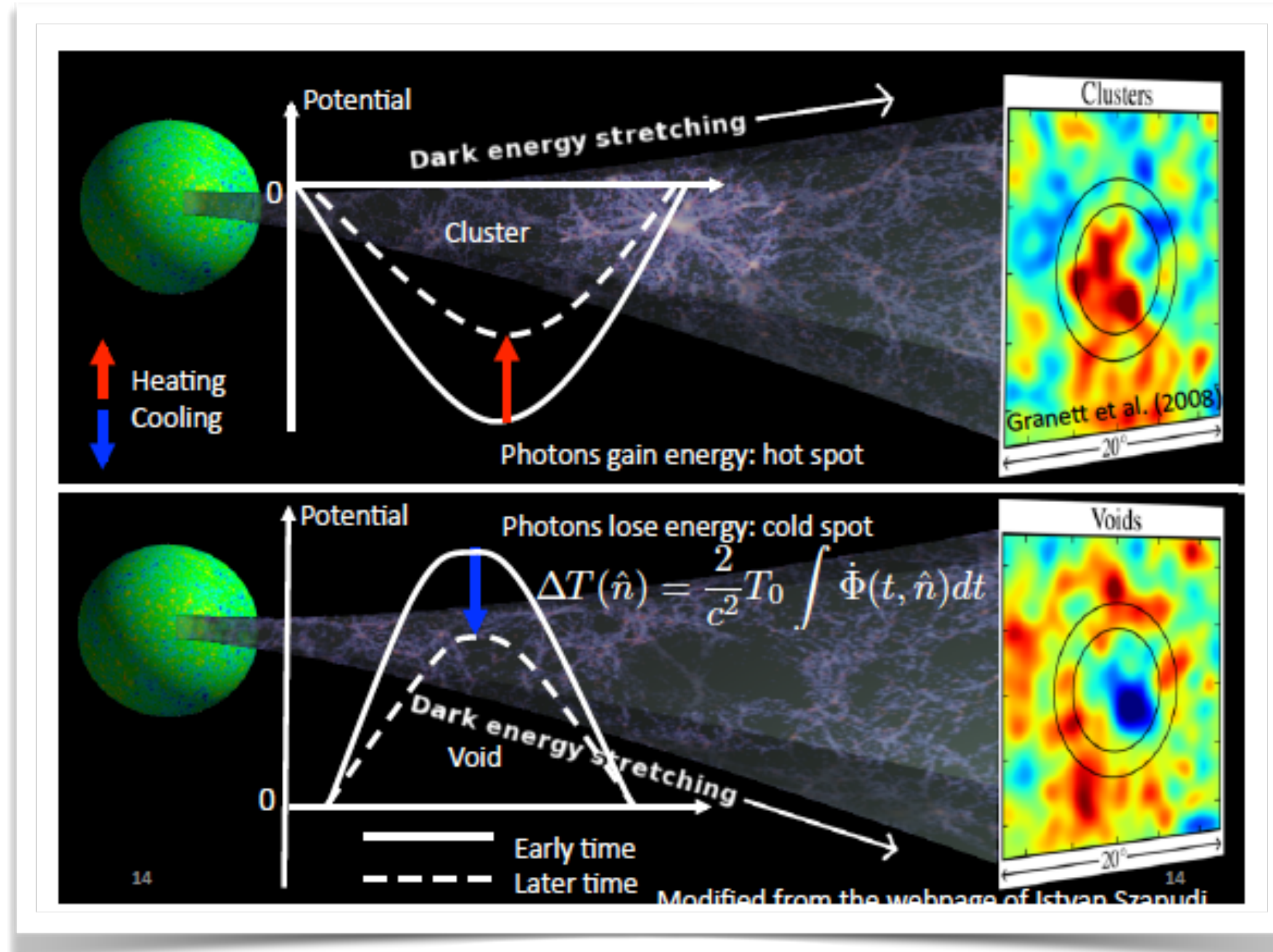
Cold Spot

1000 Mpc/h



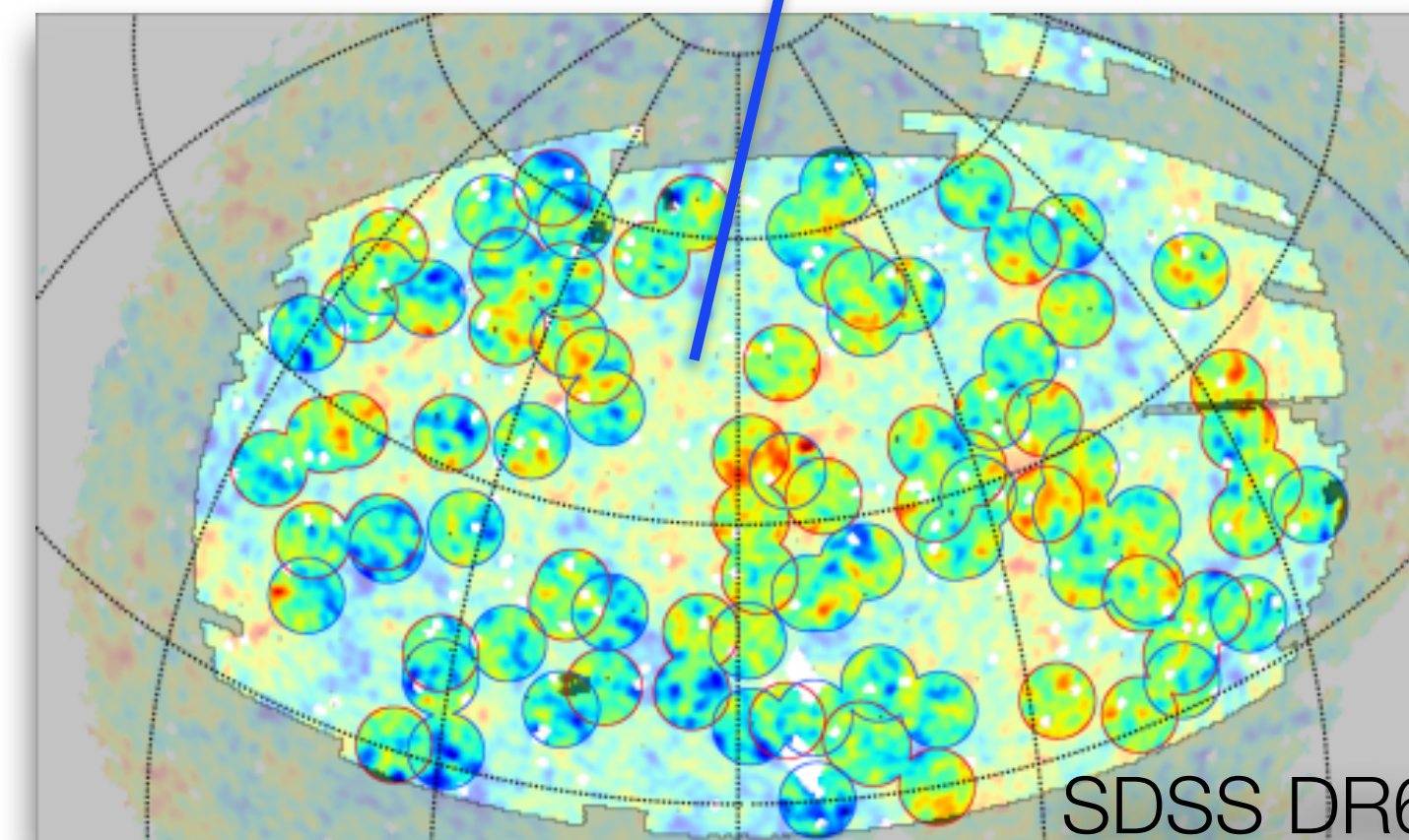
Granett et al. 2008 - ISW?

Supervoids Superclusters



Colder-than-expected imprint!

N	Radius	$\Delta T \mu\text{K}$	$\Delta T/\sigma$
30	4.0°	11.1	4.0
50	4.0°	9.6	4.4
70	4.0°	5.4	2.8
50	3.0°	8.4	3.4
50	3.5°	9.3	4.0
50	4.0°	9.6	4.4
50	4.5°	9.2	4.4
50	5.0°	7.8	3.8



Stacking at superstructure locations:

Do we have a good model for this?

Anomaly? ISW(-like)?

The integrated Sachs-Wolfe imprint of cosmic superstructures: a problem for Λ CDM

Nadathur et al. 2012 $-2 \mu\text{K}$

Seshadri Nadathur,^{a,b} Shaun Hotchkiss^c and Subir Sarkar^a

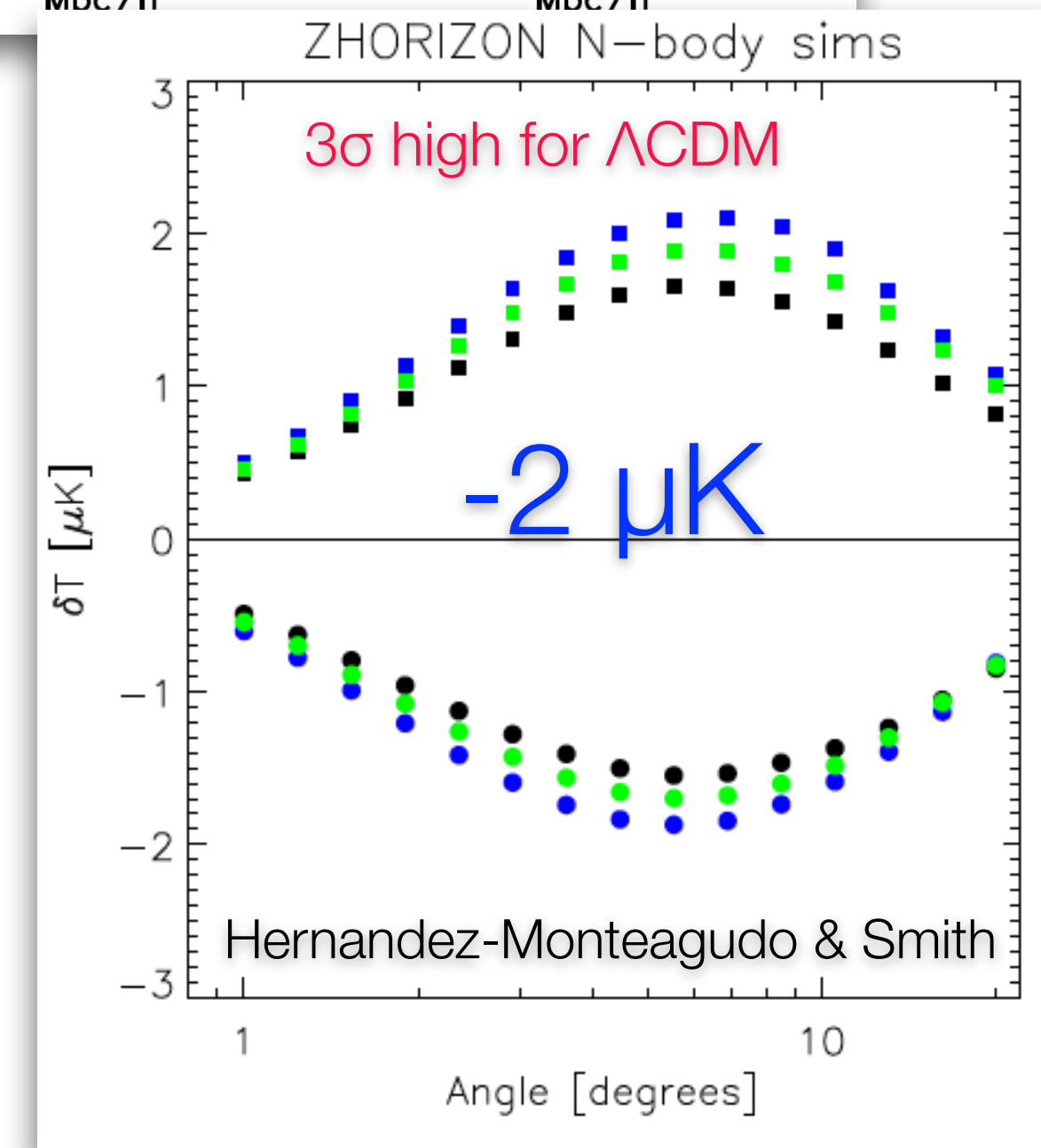
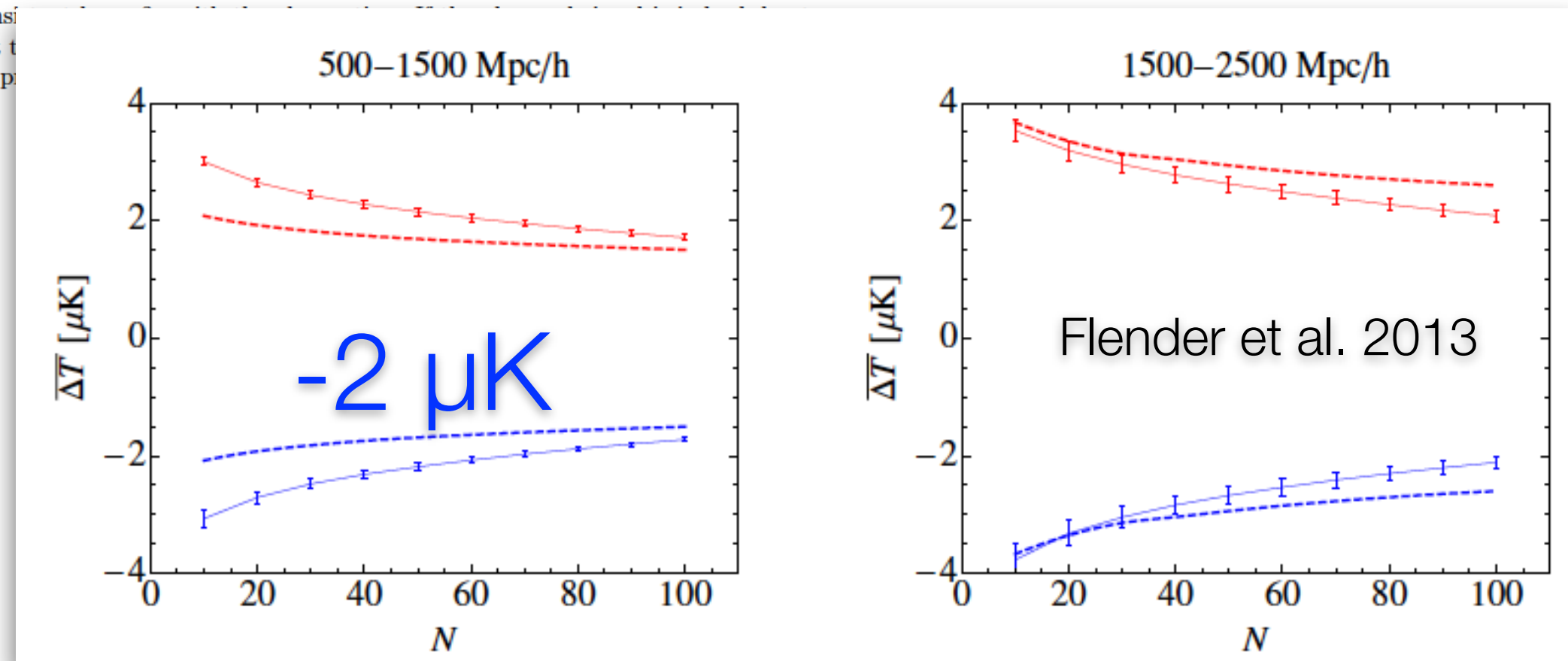
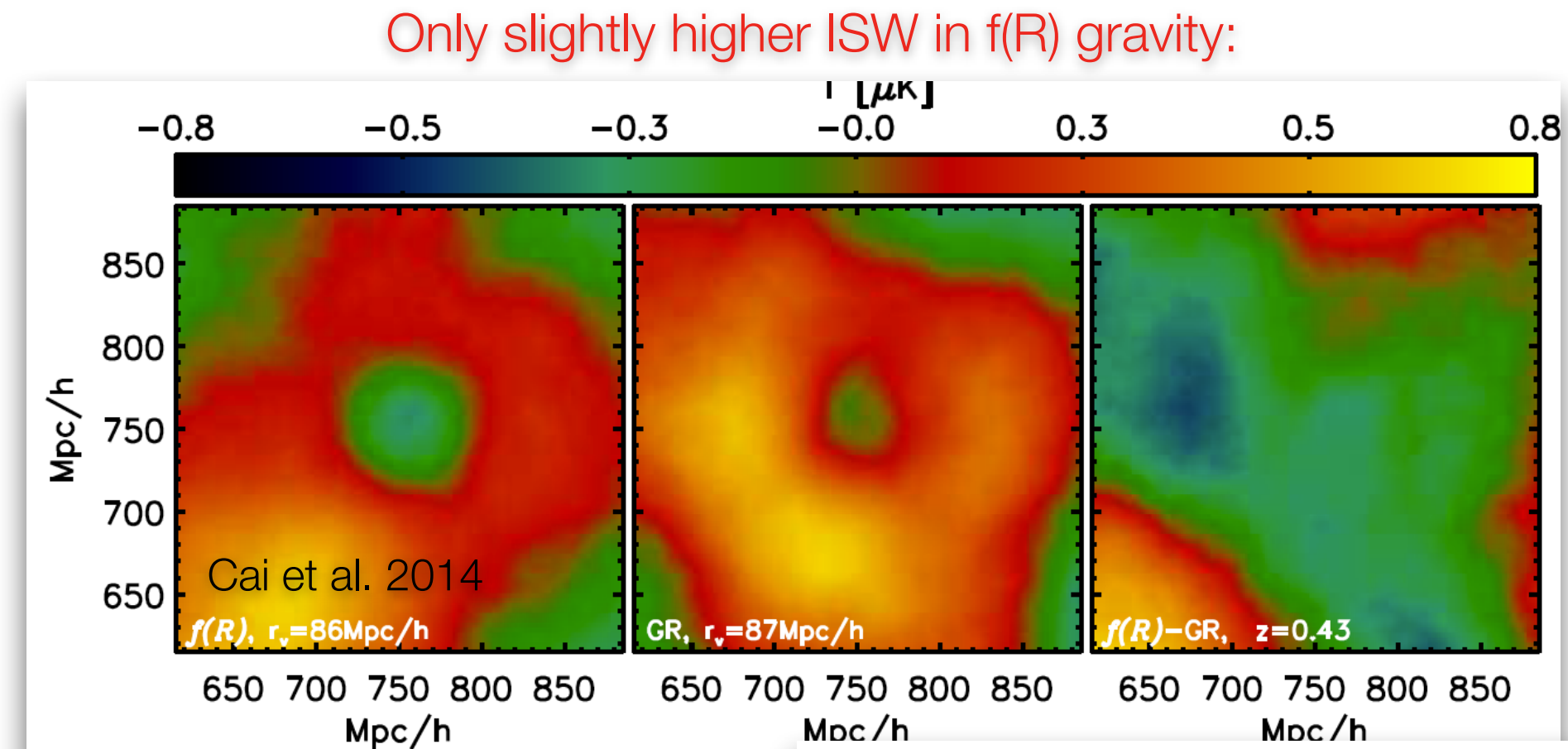
^aRudolf Peierls Centre for Theoretical Physics, University of Oxford, Oxford OX1 3NP, UK

^bFakultät für Physik, Universität Bielefeld, Postfach 100131, 33501 Bielefeld, Germany

^cDepartment of Physics, University of Helsinki and Helsinki Institute of Physics, P.O. Box 64, FIN-00014 University of Helsinki, Finland

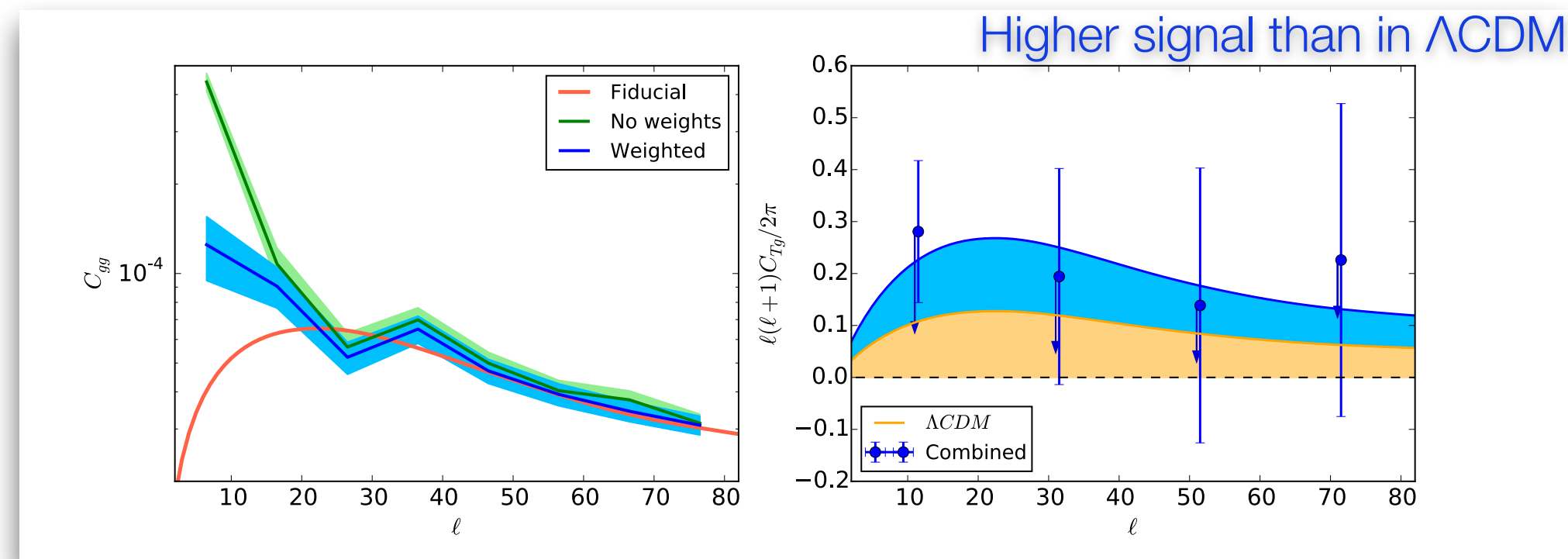
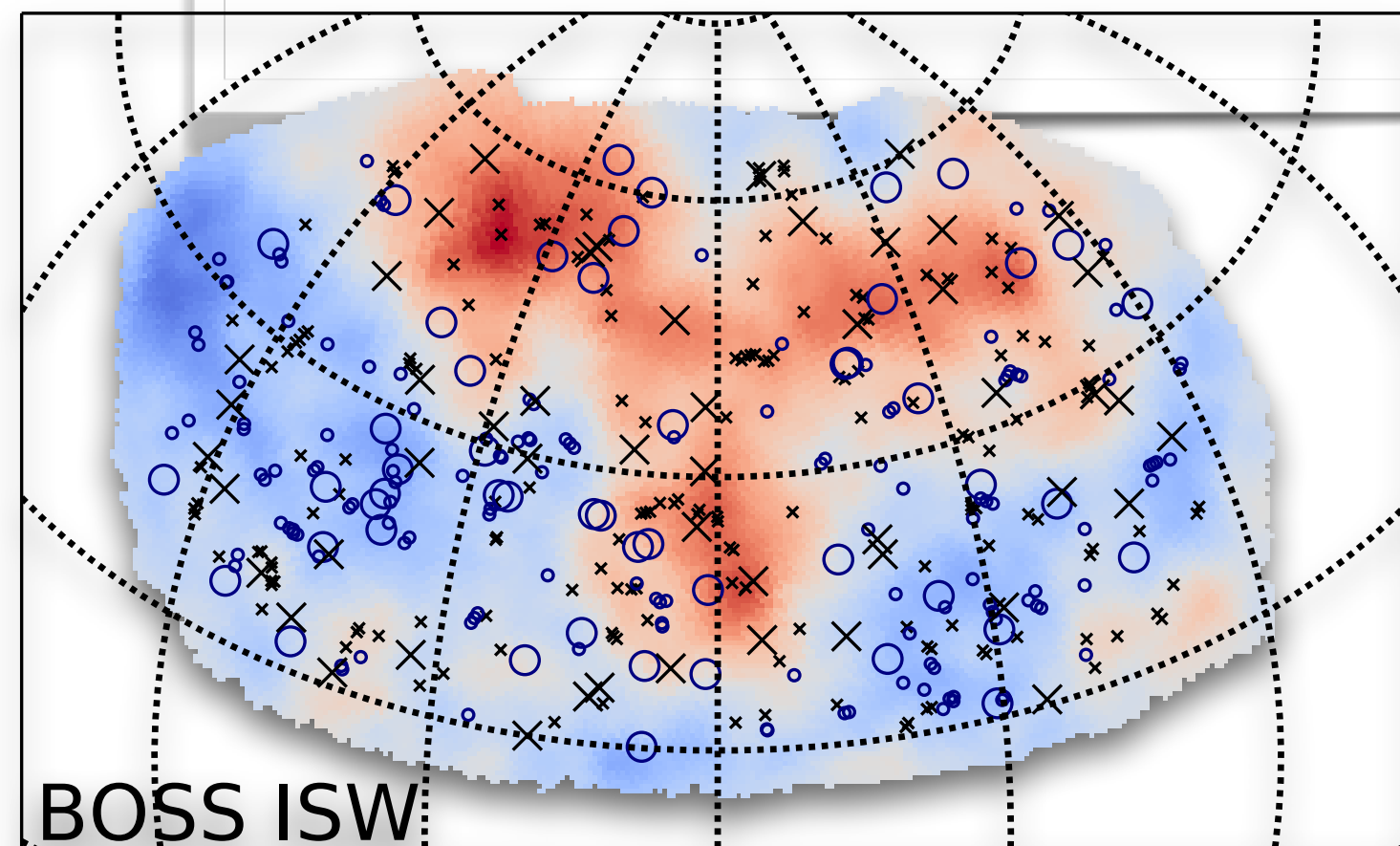
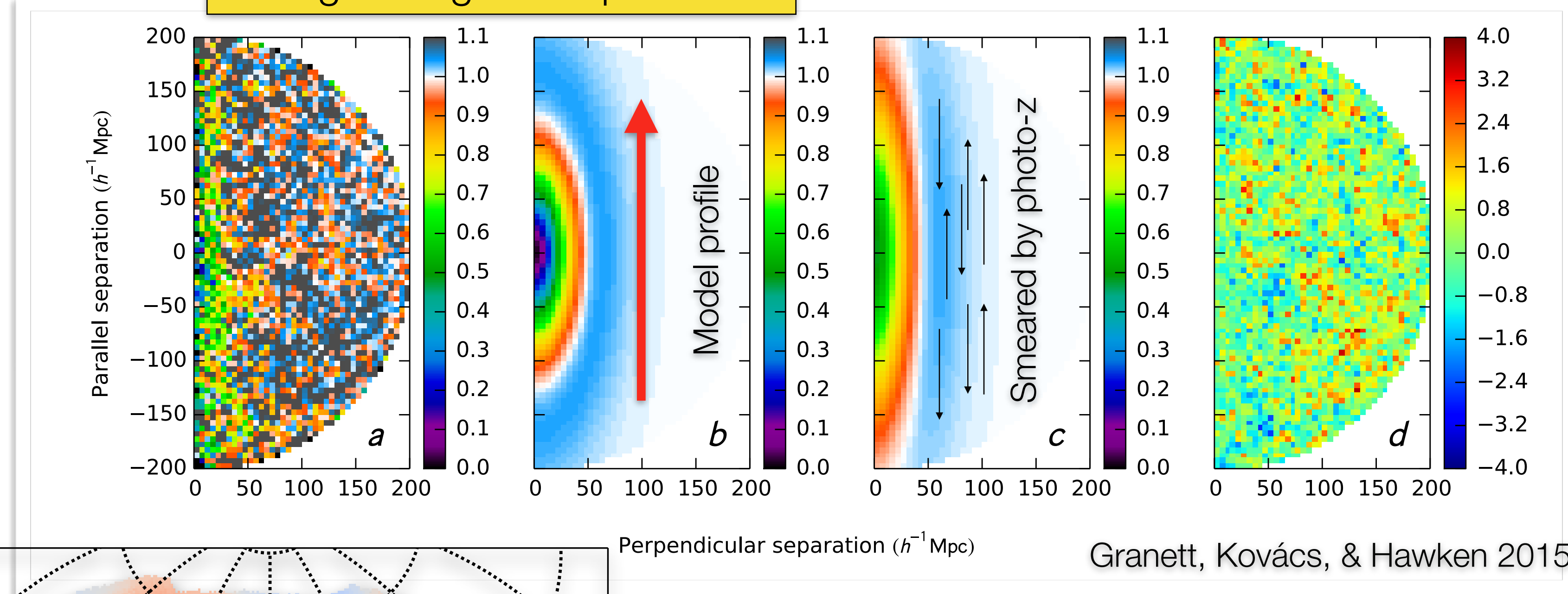
E-mail: seshadri@physik.uni-bielefeld.de, shaun.hotchkiss@helsinki.fi, s.sarkar@physics.ox.ac.uk

Abstract. A crucial diagnostic of the Λ CDM cosmological model is the integrated Sachs-Wolfe (ISW) effect of large-scale structure on the cosmic microwave background (CMB). The ISW imprint of superstructures of size $\sim 100 h^{-1}\text{Mpc}$ at redshift $z \sim 0.5$ has been detected with $> 4\sigma$ significance, however it has been noted that the signal is much larger than expected. We revisit the calculation using linear theory predictions in Λ CDM cosmology for the number density of superstructures and their radial density profile, and take possible selection effects into account. While our expected signal is larger than previous estimates, it is still inconsistent with the observed signal. We conclude that the ISW effect is much larger than expected in the Λ CDM universe than predicted.



Granett voids traced by BOSS *DR12* LRGs

Average elongation: $q = 2.6 \pm 0.4$



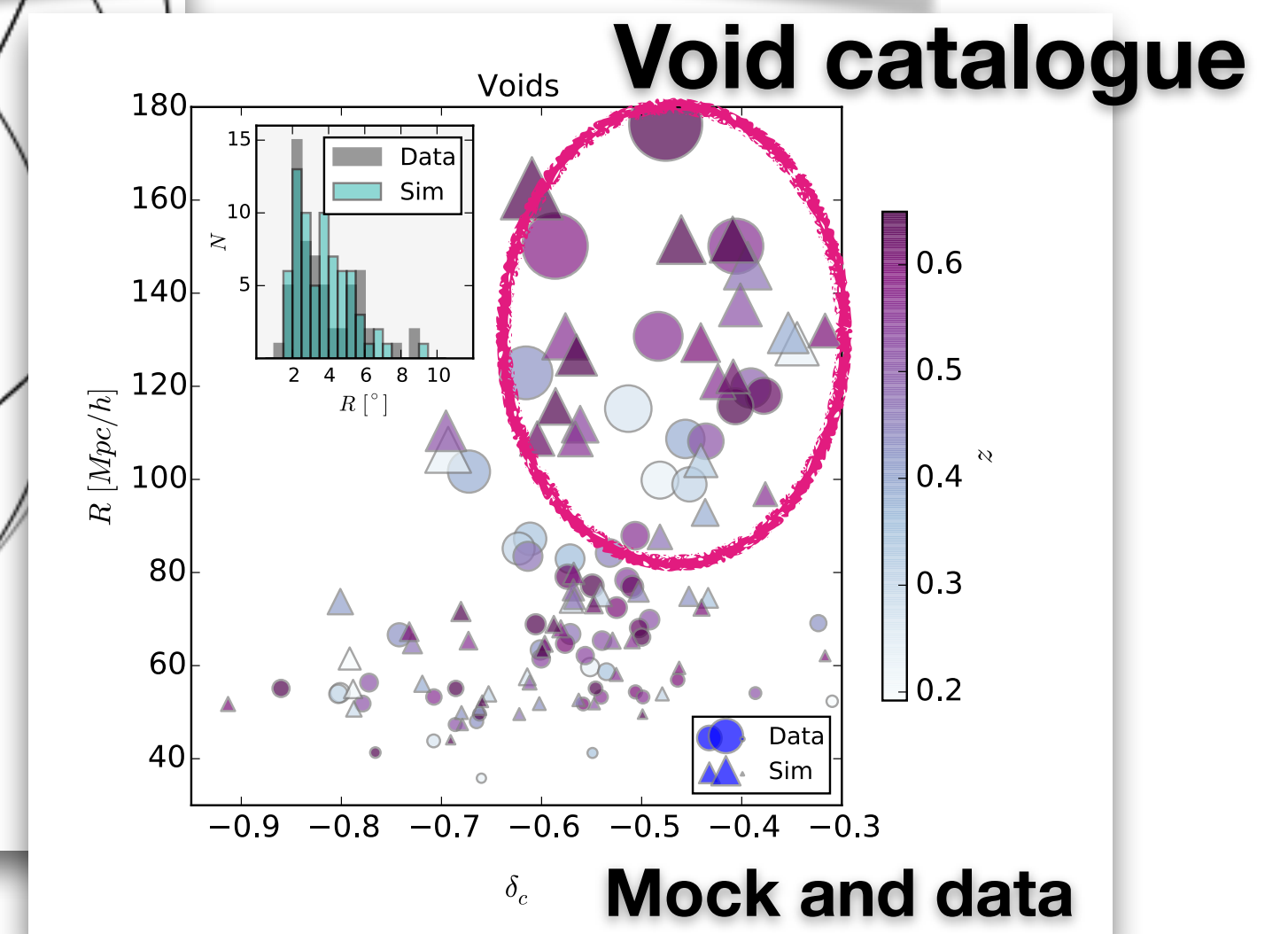
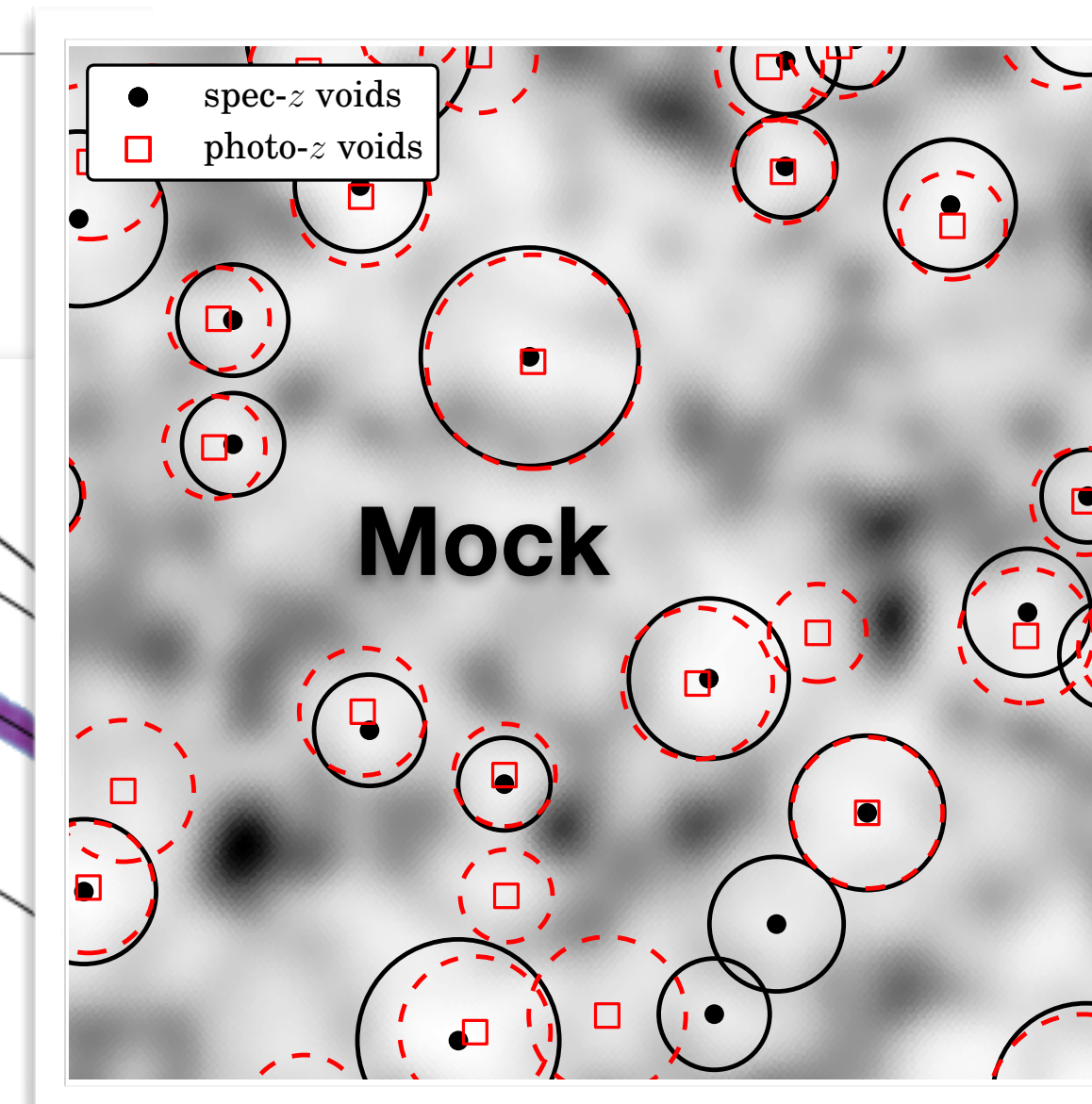
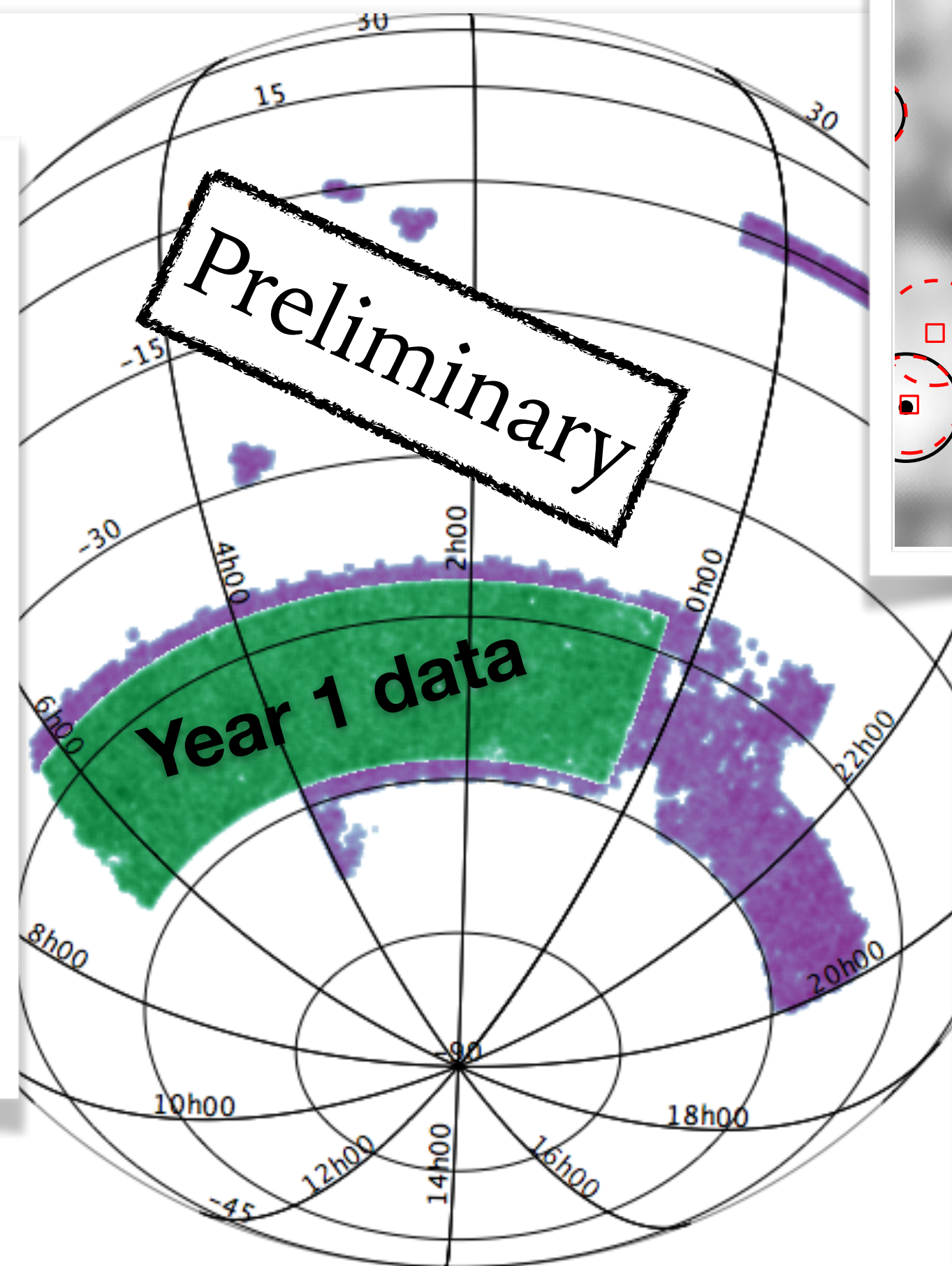
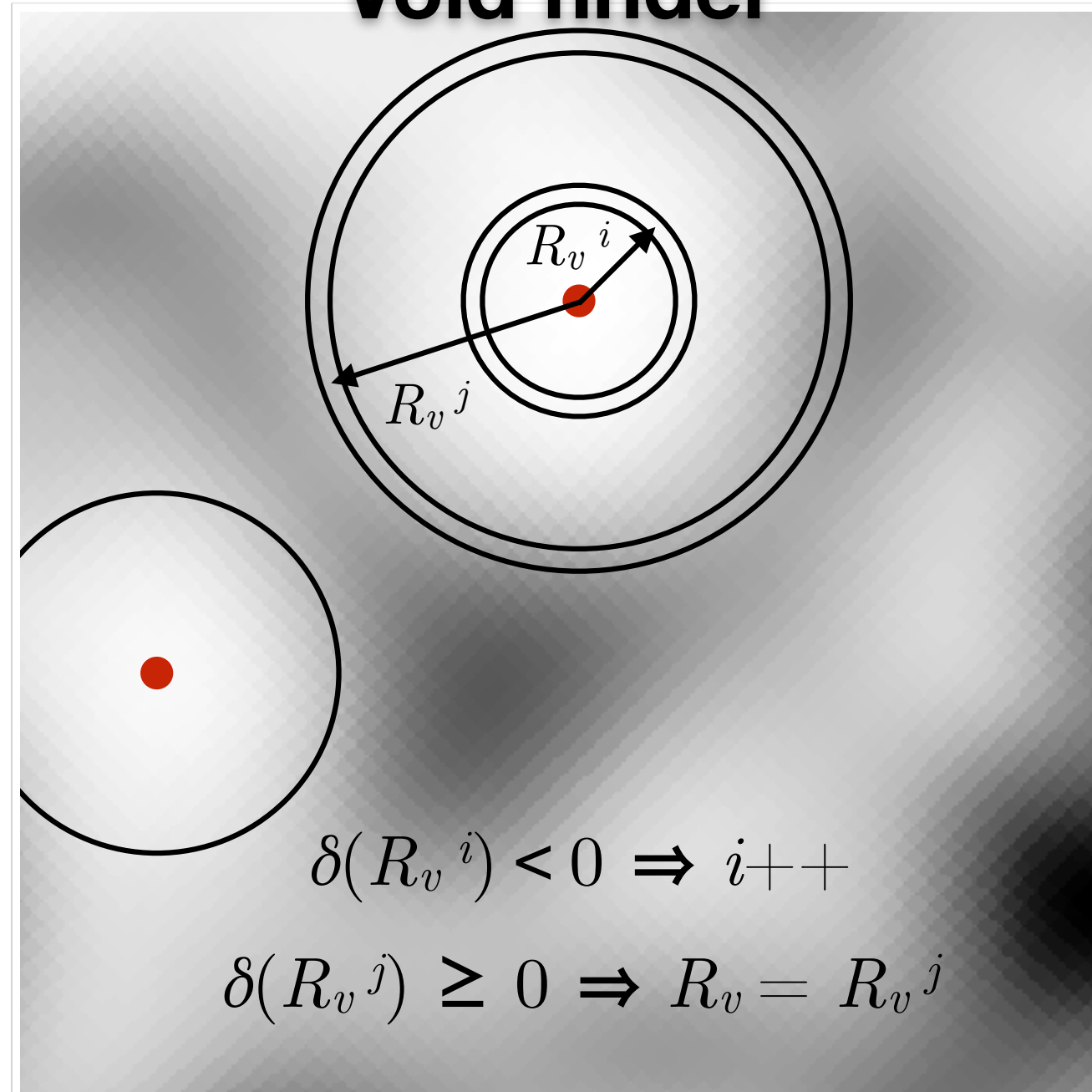
Large **photo-z** voids in DES



DARK ENERGY SURVEY

with Carles Sánchez (IFAE), Juan Garcia-Bellido, Sesh Nadathur

Void finder



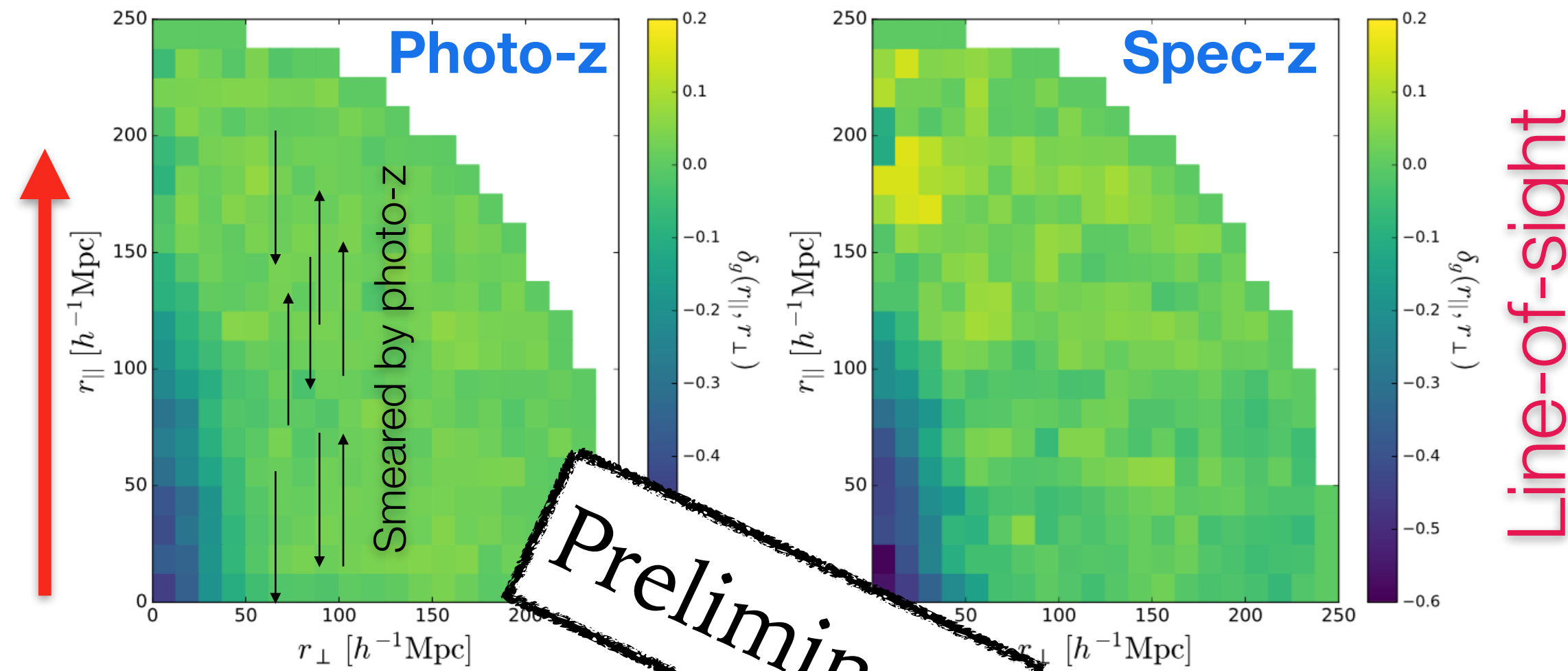
Large **photo-z** voids in DES

mocks



DARK ENERGY SURVEY

Supervoids



Superclusters

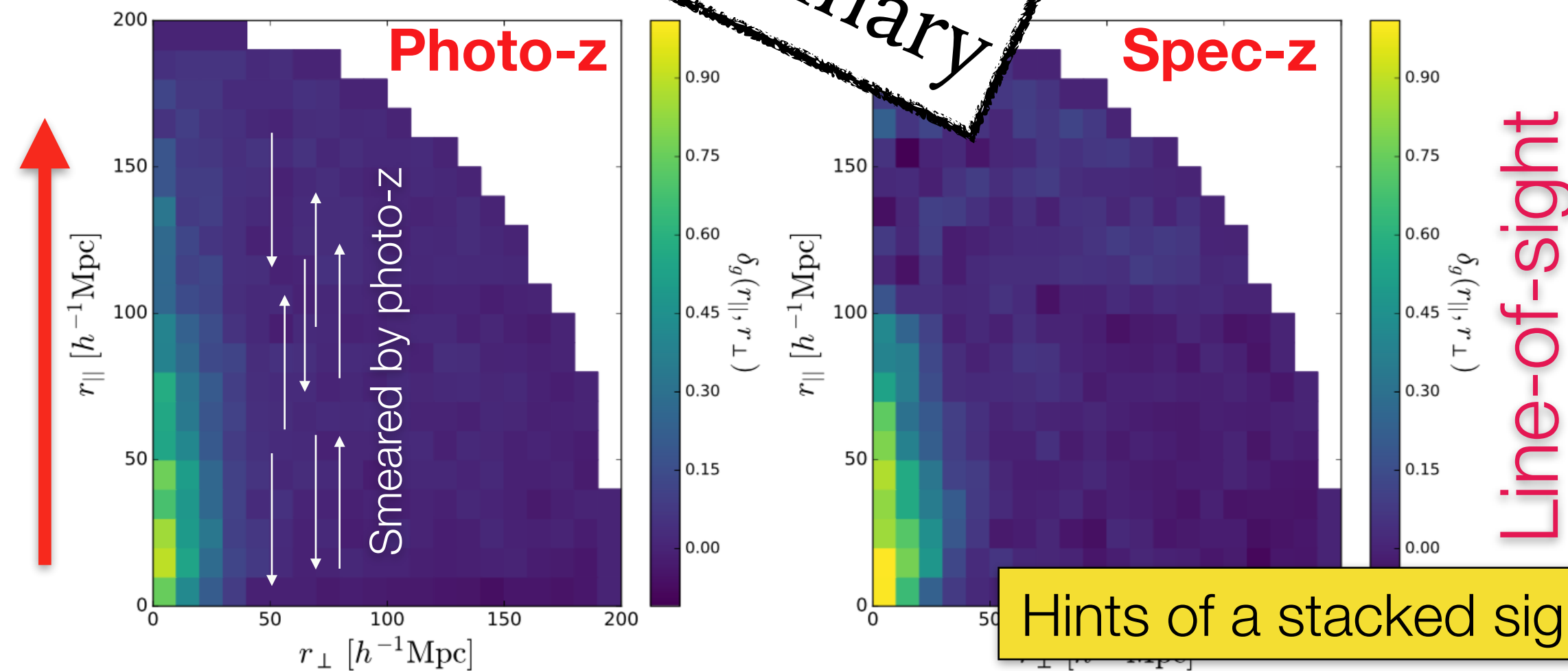
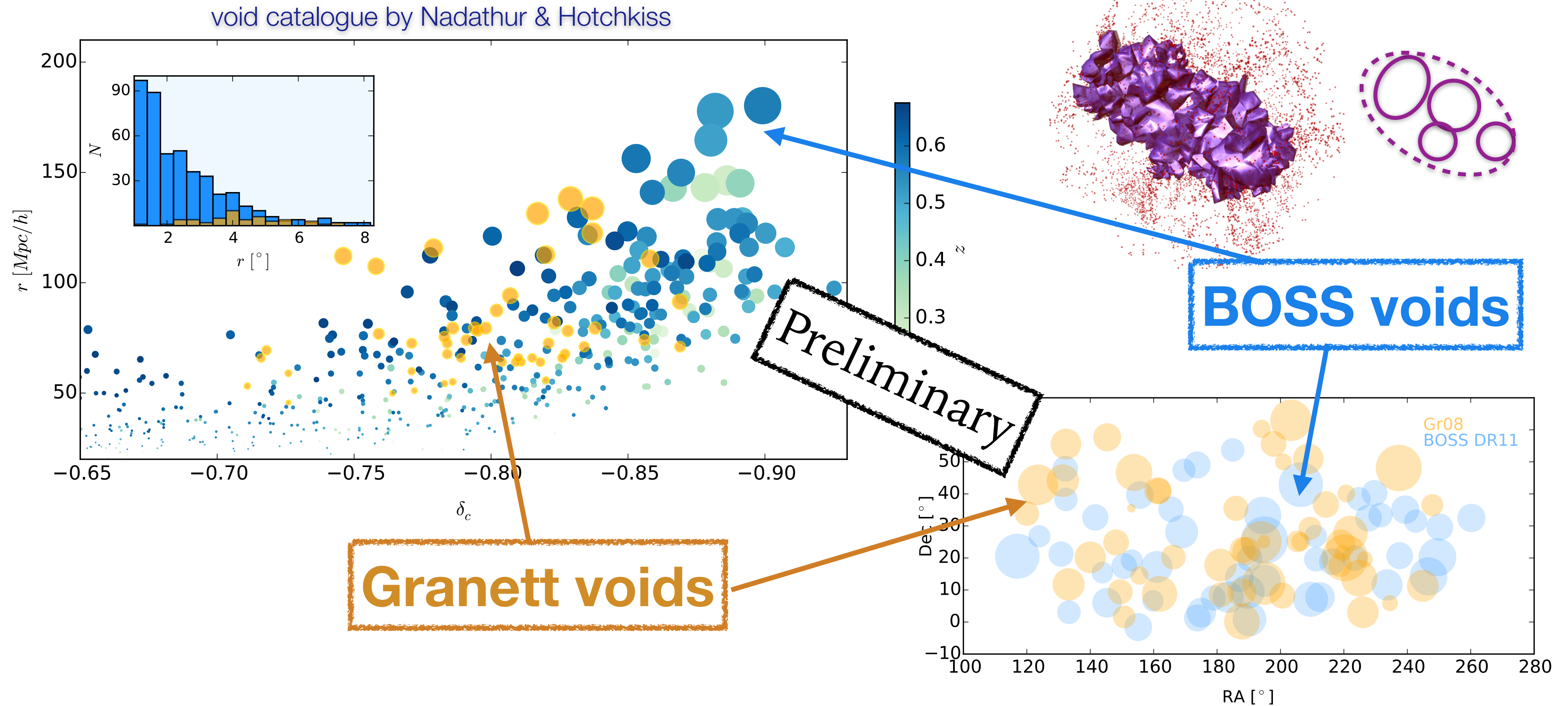


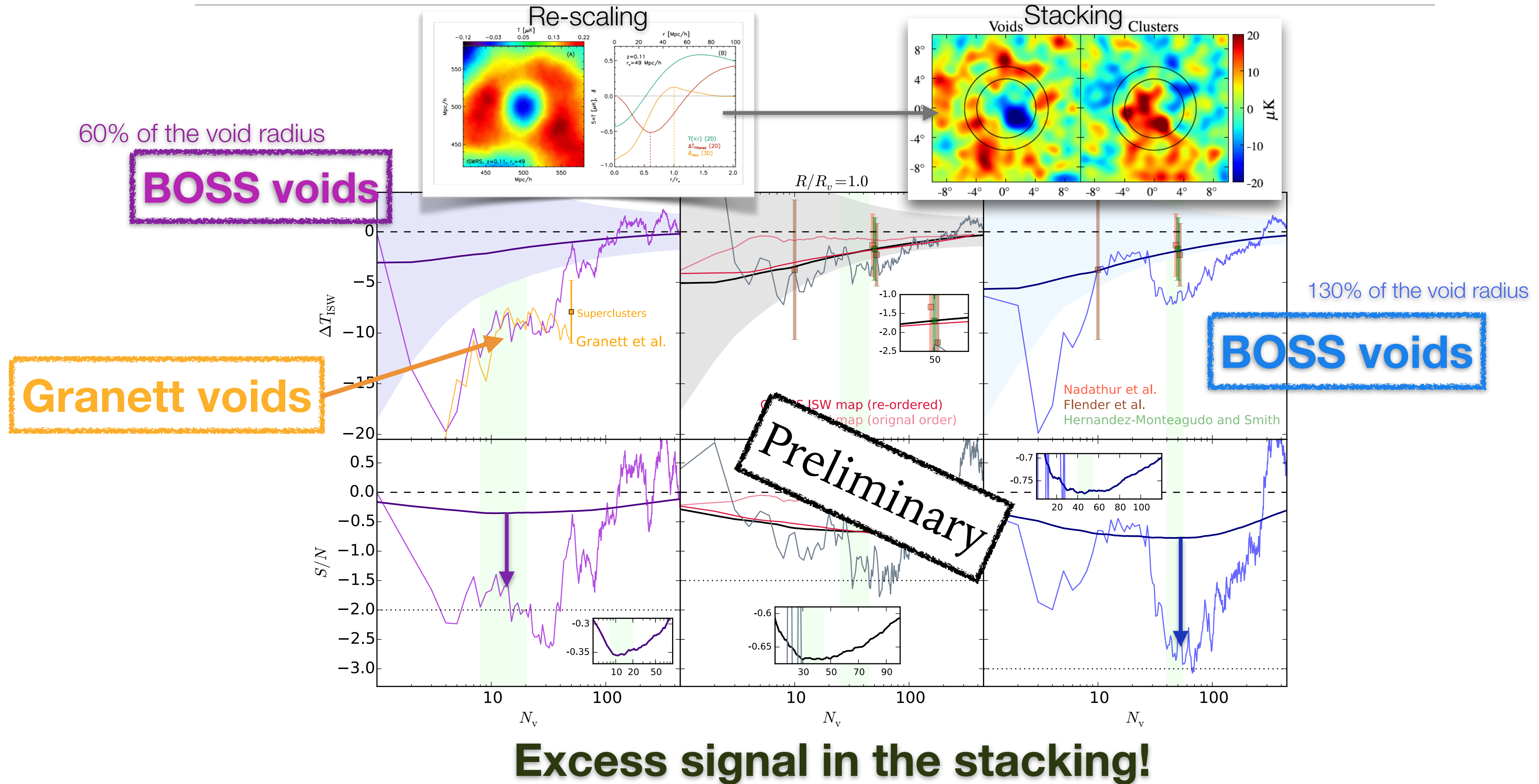
Figure 4. Line-of-sight and transverse extent of voids (*top panels*) and superclusters (*bottom panels*) as estimated in Buzzard simulations of the Y1A1 redMaGiC mock catalogue by stacking their density profiles. In both cases, the galaxy counts are inconsistent with a spherical profile, and, as expected, photo-z smearing reduces the contrast in the center in case of photo-z coordinates (*left panels*) compared to spec-zs (*right panels*).

Next step: stacking **BOSS DR11** voids

with Ben Granett, Juan Garcia-Bellido, Sesh Nadathur



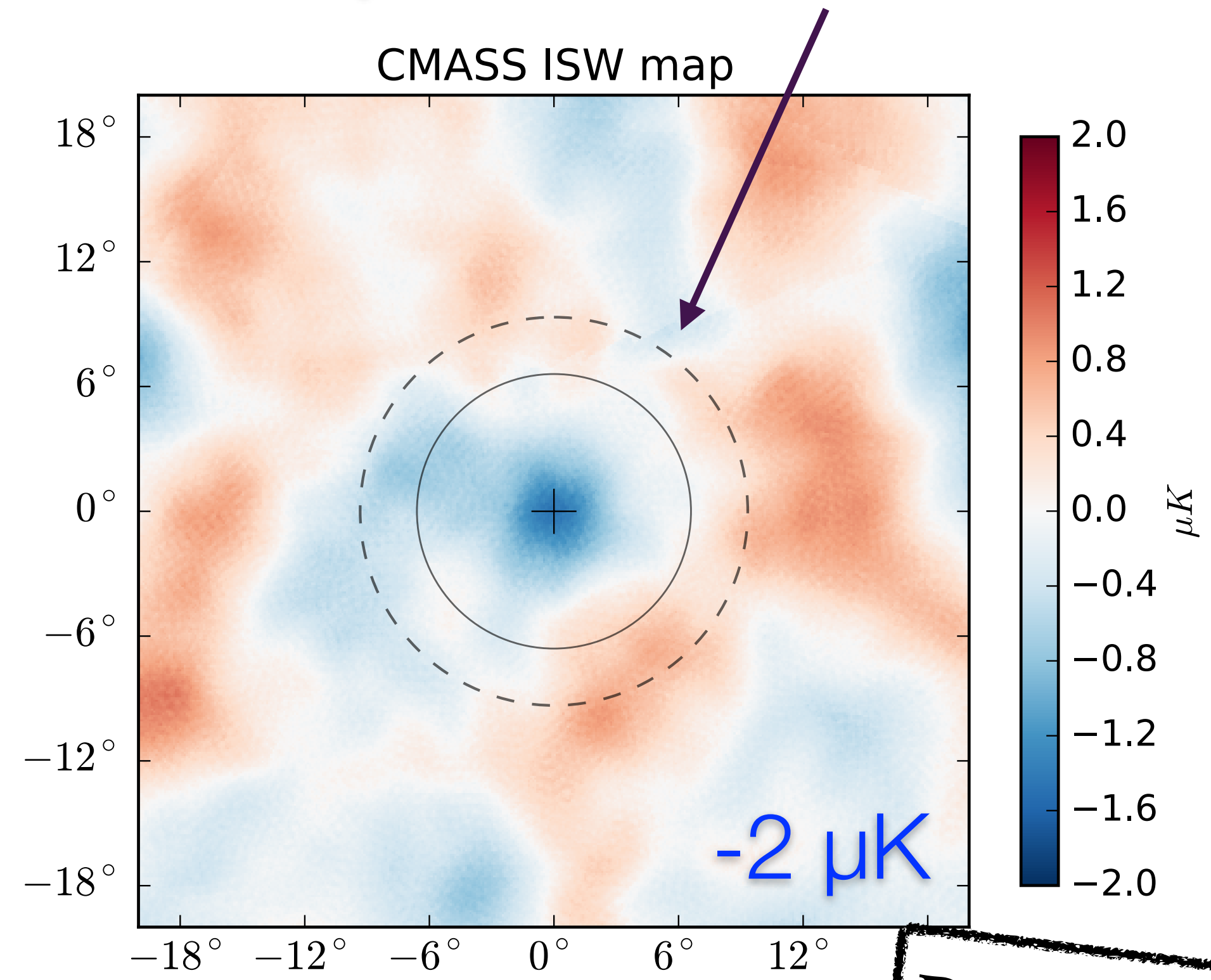
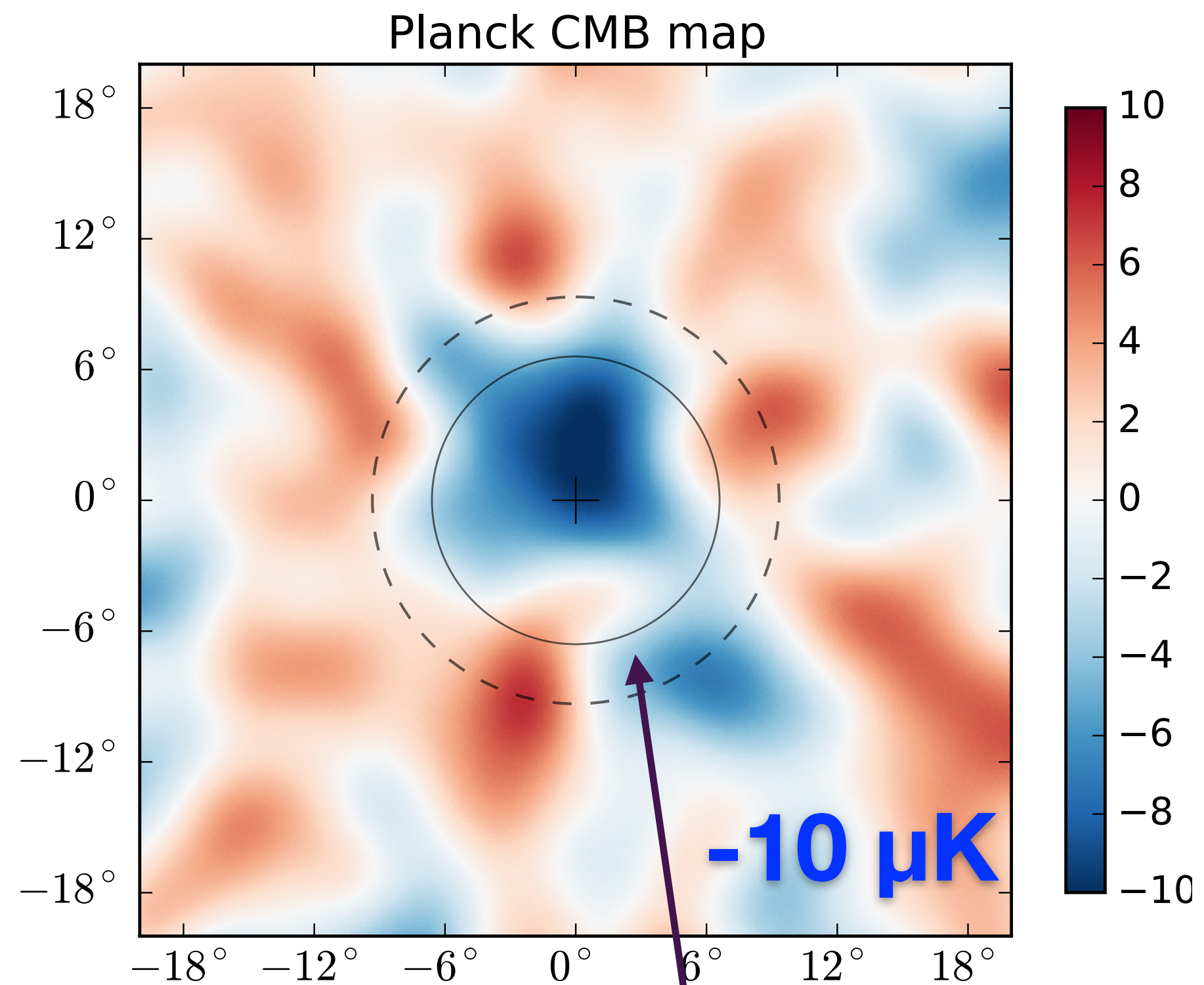
Next step: stacking **BOSS DR11** voids



Next step: stacking **BOSS DR11** voids

Kovács et al. in prep.

Moderate imprint for the reconstructed ISW map

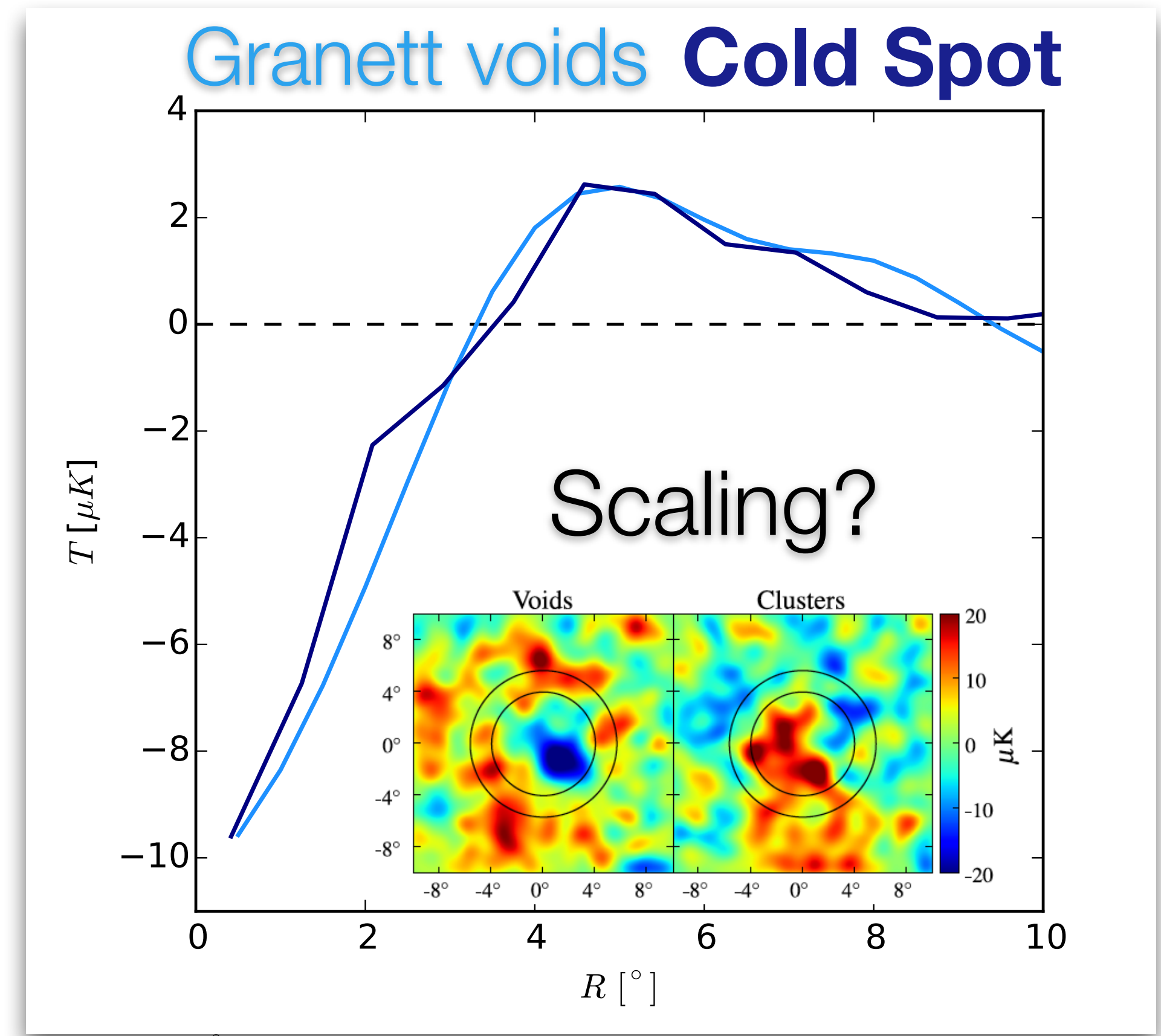


Compelling imprint for data

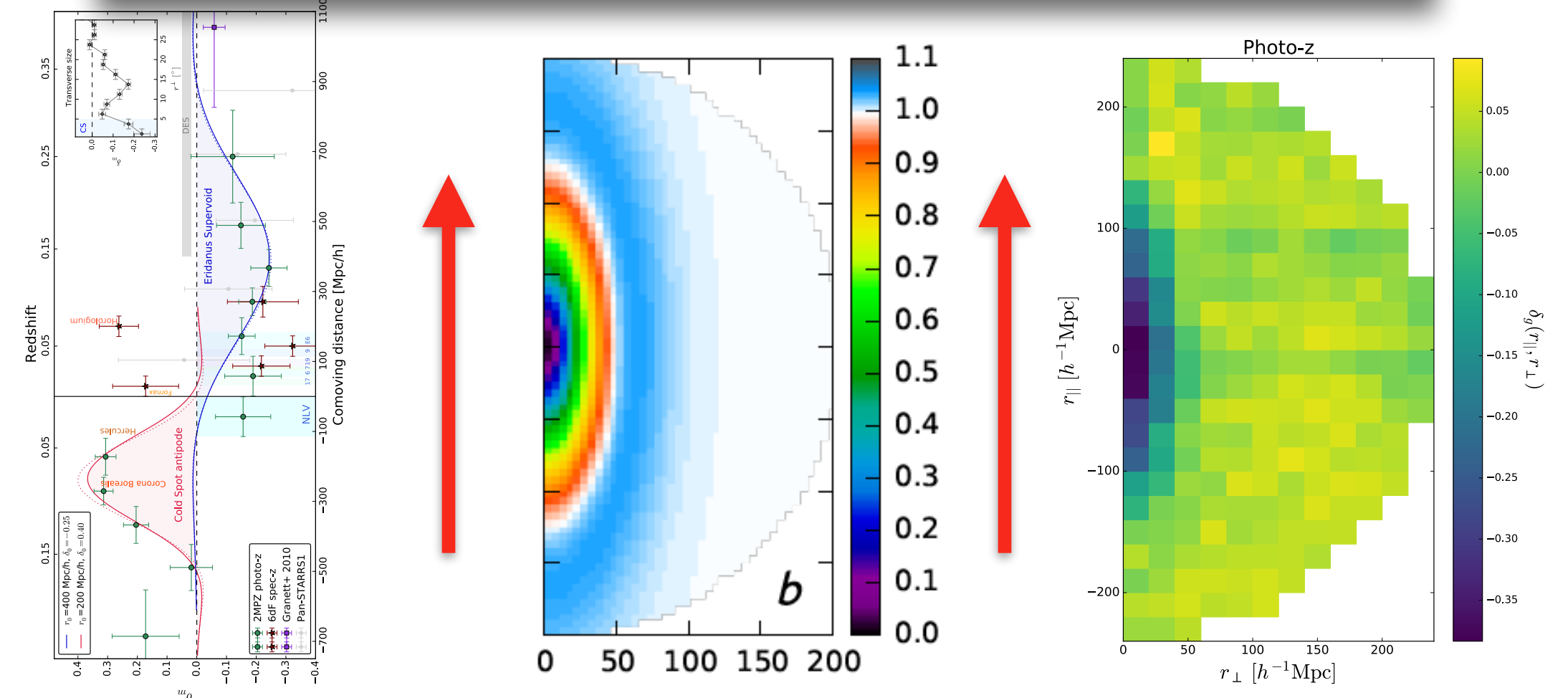
Preliminary

Summary

- the anomaly of the ISW-like Granett 2008 result is still there, the *SDSS photo-z* supervoids are **elongated**
- **elongated** supervoid detected at the Cold Spot in *WISE-PS1 photo-z* data but there is no convincing evidence for causality
- *DES* provides new data to study this outstanding issue with a special set of **elongated photo-z** voids
- *BOSS DR11* data shows unexpected cold imprint using special **merged** void samples
- New physics or coincidence?



Line-of-sight



VILA DO CONDE,
PORTUGAL,
29-31 MARCH, 2016

11th Iberian Cosmology Meeting

IBERICOS 2016

SOC ANA ACHÚCARRO (LEIDEN/BILBAO),
FERNANDO ATRIO-BARANDELA (SALAMANCA),
MAR BASTERO-GIL (GRANADA), JUAN GARCIA-
-BELLIDO (MADRID), RUTH LAZKOZ (BILBAO),
CARLOS MARTINS (PORTO), JOSÉ PEDRO
MIMOSO (LISBON), DAVID MOTA (OSLO)

LOC ANA CATARINA LEITE, CARLOS MARTINS
(CHAIR), FERNANDO MOUCHEREK, PAULO
PEIXOTO (SYSADMIN), ANA MARTA PINHO,
IVAN RYBAK, ELSA SILVA (ADMIN)

SERIES OF MEETINGS WHICH AIM
TO ENCOURAGE INTERACTIONS
AND COLLABORATIONS BETWEEN
RESEARCHERS WORKING IN
COSMOLOGY AND RELATED
AREAS IN PORTUGAL AND SPAIN.

www.iastro.pt/ibericos2016



Clustering of Lagrangian Halos

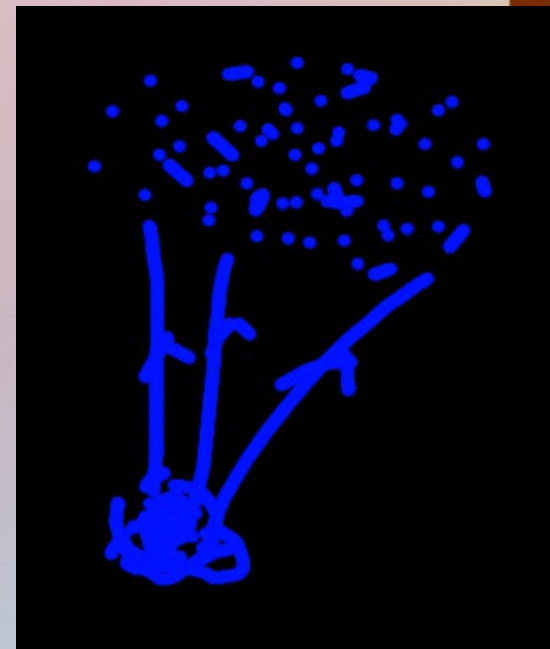
Kwan Chuen Chan
ICE, Barcelona

Porto, 29 Mar 2016

KCC, R K Sheth and R Scoccimarro, 1511.01909
KCC, R K Sheth and R Scoccimarro, to appear

Lagrangian halos

- Final Eulerian halos are hard because of nonlinear evolution
- Theoretical modeling often starts in Lagrangian space. Modeling is easier as DM is Gaussian
- But what determine a Lagrangian halos in theory? Only density matter or other variables as well? Pioneering work by BBKS 1986.
- Numerically, reverse the evolution, tracing particles in the Eulerian halos back to initial conditions, the position of the Lagrangian halo is estimated by the CM position of the constituent particles



Lagrangian window function

- The Lagrangian halo profile is often assumed to be a top hat filter
- The window function selects a fraction of the DM particles to form a Lagrangian halo, appear everywhere in Lagrangian modeling of halos, but its functional form is unconstrained
- Used to compute spectrum moments of the power spectrum. Previously top-hat for zero order, Gaussian for higher order.

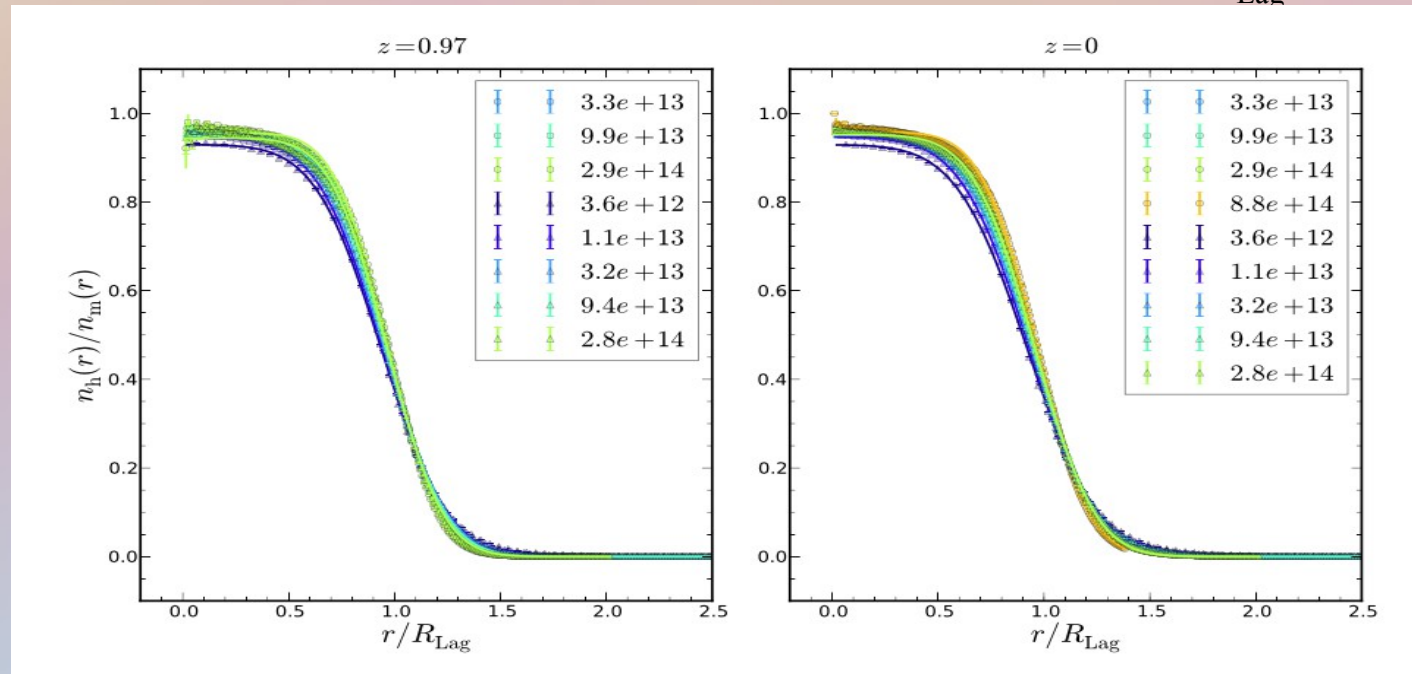
$$s_j = \int \frac{dk}{2\pi^2} k^{2(1+j)} P_m(k) W^2(kR)$$

Constructing Lagrangian window

- Stacking the Lagrangian profiles together to get the spherically averaged profile
- The window function is proportional to the probability that a particle at distance r is incorporated into the Lagrangian halo

$$N = \frac{4\pi}{3} \bar{n}_m R_{\text{Lag}}^3, \quad W(r) = \frac{3p_h(r)}{4\pi R_{\text{Lag}}^3}$$

- More extended than a top-hat, less diffuse than a Gaussian
- Quite universal in mass and redshift when plotted against R_{Lag}



$$W(kR_{\text{Lag}}) = W_{\text{TH}}(kR_{\text{Lag}})W_{\text{G}}\left(\frac{\sqrt{f}kR_{\text{Lag}}}{5}\right)$$

Lagrangian constraints and consistency relations

- What determines a Lagrangian halos?
- Lagrangian halos can be defined by imposing some constraints on the smoothed dark matter density field
- In peak model, halos are postulated to be peaks in the density field smoothed by the window function satisfying

$$\delta_R \geq \delta_c, \quad \nabla \delta_R = \mathbf{0}, \quad \nabla^2 \delta_R < 0$$

BBKS 1986

- Given some points satisfying certain constraints, the correlation between some large-scale field and these points can reveal the constraints, i.e. the halo formation physics

Lagrangian constraint and consistency relations

When the random variable C is constrained to be some specific values \mathcal{C} , the conditional mean of the large-scale field Δ is

$$\langle \Delta | C = \mathcal{C} \rangle = \langle \Delta C \rangle_j \langle CC \rangle^{-1}_{jk} \mathcal{C}_k,$$

where the vector $\langle \Delta C \rangle$ denotes the cross correlation between Δ and the constraint variables, and $\langle CC \rangle$ is the covariance matrix between the constraint variables. We define the linear bias coefficients as

$$\langle \Delta | C = \mathcal{C} \rangle = \frac{\langle \Delta C \rangle_j}{\langle CC \rangle_{1j}} \sqrt{s_0} b_j^1,$$

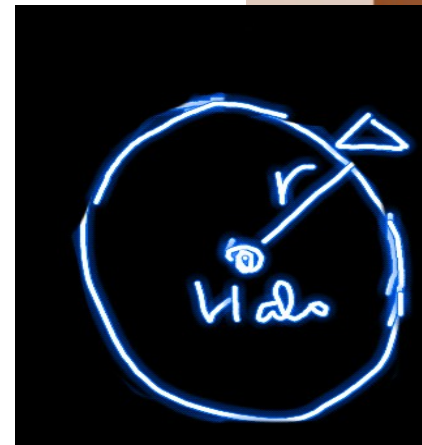
where b_j^1 is the j^{th} linear bias coefficient

$$b_j^1 = \frac{1}{\sqrt{s_0}} \langle CC \rangle_{1j} \langle CC \rangle^{-1}_{jk} \mathcal{C}_k.$$

In particular, we can invert this equation to express \mathcal{C}_k in terms of b_j^1

$$\mathcal{C}_k = \langle CC \rangle_{kj} \frac{\sqrt{s_0} b_j^1}{\langle CC \rangle_{1j}}.$$

There are n relations existing among the bias parameters, where n is the dimension of $\langle CC \rangle$, and they simply reflect the underlying constraints for halo formation.



See also Musso Paranjape & Sheth 2012
Paranjape, Sheth & Desjacques 2013

First consistency relation

The first of these hierarchy of consistency relations is for \mathcal{C}_1 and it is given by

$$\sum_j b_j^1 = \frac{\mathcal{C}_1}{\sqrt{s_0}}.$$

We now proceed to prove it. We first write the covariance matrix in the block matrix form as

$$\langle CC \rangle = \begin{pmatrix} a_{11} & \mathbf{a}^T \\ \mathbf{a} & A \end{pmatrix},$$

where \mathbf{a} is an $n - 1$ dimension column vector, and A is a $(n - 1) \times (n - 1)$ symmetric matrix. The inverse of a block matrix is well-known and it is given by

$$\langle CC \rangle^{-1} = \begin{pmatrix} \frac{1}{\alpha} & -\frac{1}{\alpha} \mathbf{a}^T A^{-1} \\ -\frac{1}{\alpha} A^{-1} \mathbf{a} & A^{-1} + \frac{1}{\alpha} A^{-1} \mathbf{a} \mathbf{a}^T A^{-1} \end{pmatrix},$$

where $\alpha = a_{11} - \mathbf{a}^T A^{-1} \mathbf{a}$. Plugging this into the b_j^1 , it follows that $\sum_j b_j^1$ indeed gives $\mathcal{C}_1 / \sqrt{s_0}$.

Example, n=2

Suppose $C = (\nu, u)$ with, in Fourier space,

$$\nu = W \frac{\delta_m}{\sqrt{s_0}}, \quad u = \frac{1}{\sqrt{s_u}} \frac{dW}{ds_0} \delta_m$$

Then

$$\langle CC \rangle = \begin{pmatrix} 1 & \langle \nu u \rangle \\ \langle \nu u \rangle & 1 \end{pmatrix}.$$

The bias expansion is given by

$$\langle \Delta | C = (\nu_c, u_c) \rangle = \left[W b_1^1 + 2 \frac{dW}{d \ln s_0} b_2^1 \right] \langle \Delta \delta_m \rangle,$$

with the bias parameters being

$$b_1^1 = \frac{\nu_c - \langle \nu u \rangle u_c}{\sqrt{s_0} (1 - \langle \nu u \rangle^2)},$$
$$b_2^1 = \frac{\langle \nu u \rangle (u_c - \langle \nu u \rangle \nu_c)}{\sqrt{s_0} (1 - \langle \nu u \rangle^2)}.$$

The consistency relations read

$$\begin{pmatrix} \nu_c \\ u_c \end{pmatrix} = \sqrt{s_0} \begin{pmatrix} b_1^1 + b_2^1 \\ \langle \nu u \rangle b_1^1 + \frac{1}{\langle \nu u \rangle} b_2^1 \end{pmatrix}.$$

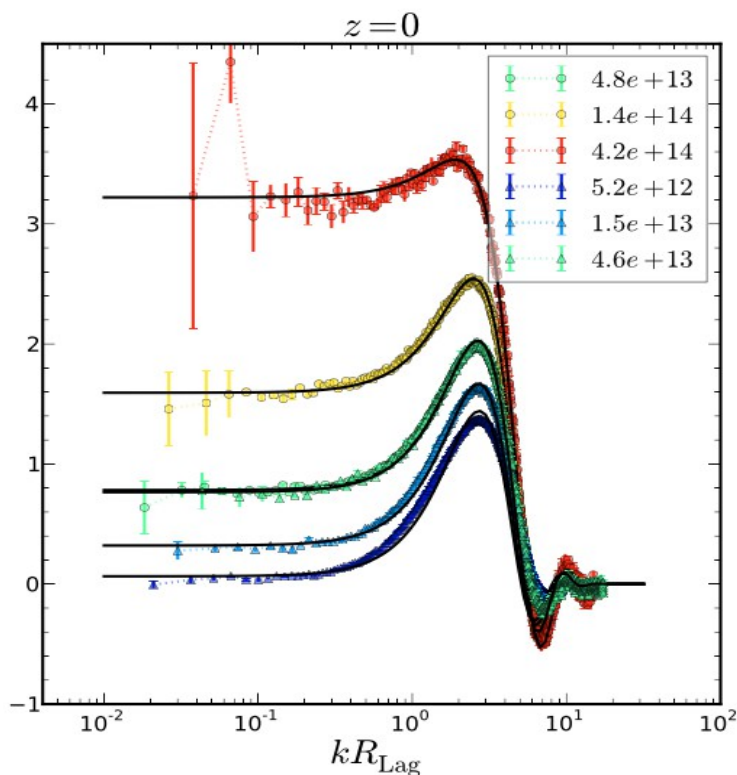
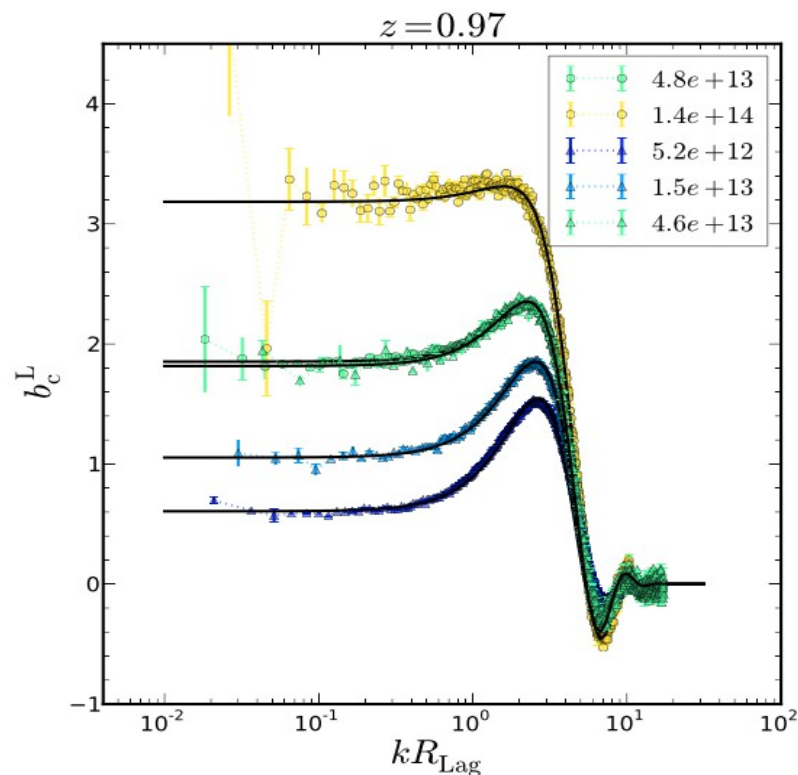
Cross Lagrangian bias parameters

- Cross bias parameter

$$b_c^L(k, z) = \frac{D(z_1)}{D(0)} \left(\frac{P_c}{P_m} - 1 \right)$$

- A simple model with 2 constrains, threshold and first crossing condition

$$b_{\text{eff}}(k) = b_{10} W(k) + 2b_{01} \frac{dW(k)}{d \ln s_0}, \quad \text{Musso \& Sheth 2012}$$

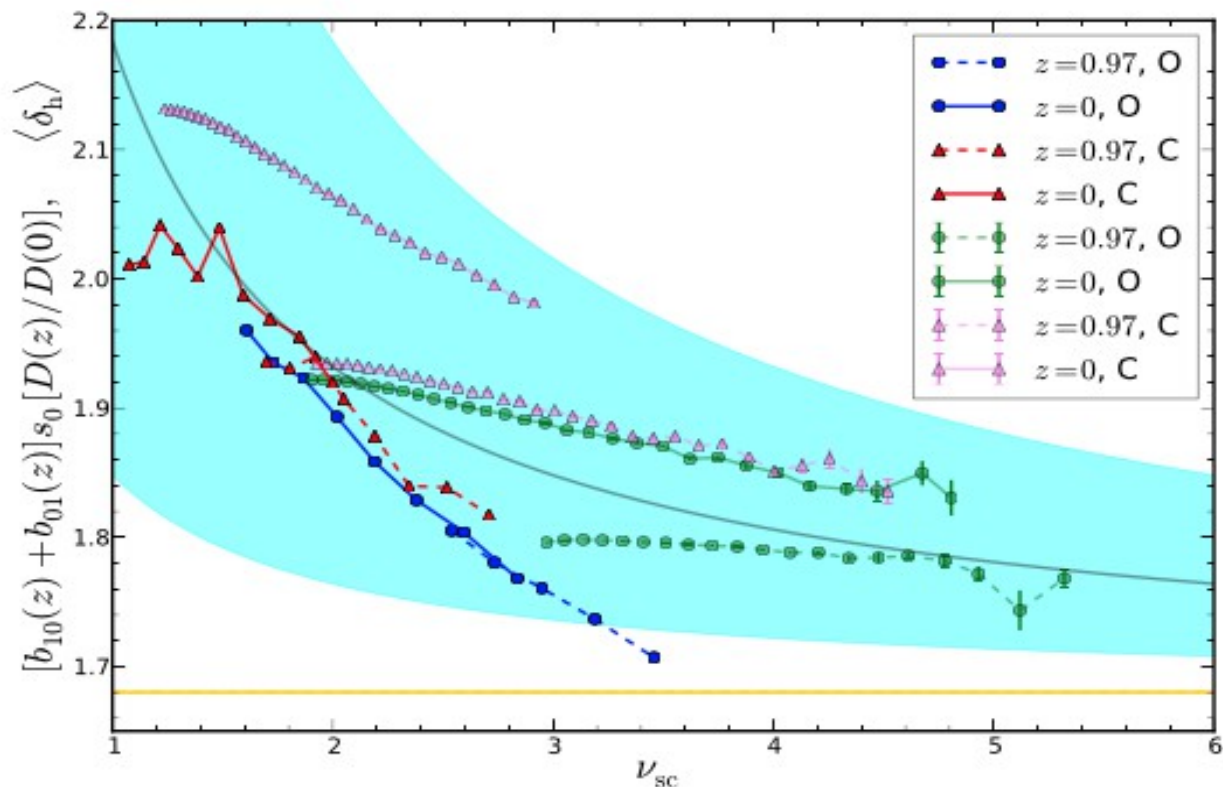


Checking the first consistency relation

- For the first time, we can extract the halo formation physics using the clustering properties of the halos. i.e. the bias

$$b_{10} + b_{01} = \frac{\delta_c(z)}{s_0}$$

- The direct and consistency relation estimate use 1-point and 2-point statistics respectively.



Summary

- We have accurately measured the window function of Lagrangian halo. It is the starting point for accurate prediction in Lagrangian space.
- With the effective window function, the excursion set bias provides a good fit to the Lagrangian cross bias parameter.
- Using the bias parameters, we check the consistency relations for the Lagrangian bias. For the first time we demonstrate the possibility to use clustering properties, i.e. bias to extract halo formation physics.

VILA DO CONDE,
PORTUGAL,
29-31 MARCH, 2016

11th Iberian Cosmology Meeting

IBERICOS 2016

SOC ANA ACHÚCARRO (LEIDEN/BILBAO),
FERNANDO ATRIO-BARANDELA (SALAMANCA),
MAR BASTERO-GIL (GRANADA), JUAN GARCIA-
BELLIDO (MADRID), RUTH LAZKOZ (BILBAO),
CARLOS MARTINS (PORTO), JOSÉ PEDRO
MIMOSO (LISBON), DAVID MOTA (OSLO)

LOC ANA CATARINA LEITE, CARLOS MARTINS
(CHAIR), FERNANDO MOUCHEREK, PAULO
PEIXOTO (SYSADMIN), ANA MARTA PINHO,
IVAN RYBAK, ELSA SILVA (ADMIN)

SERIES OF MEETINGS WHICH AIM
TO ENCOURAGE INTERACTIONS
AND COLLABORATIONS BETWEEN
RESEARCHERS WORKING IN
COSMOLOGY AND RELATED
AREAS IN PORTUGAL AND SPAIN.

www.iastro.pt/ibericos2016



***THE AMAZING WORLD OF
Effective Field Theory of Large
Scale Structures &
Redshift Space Distortions***

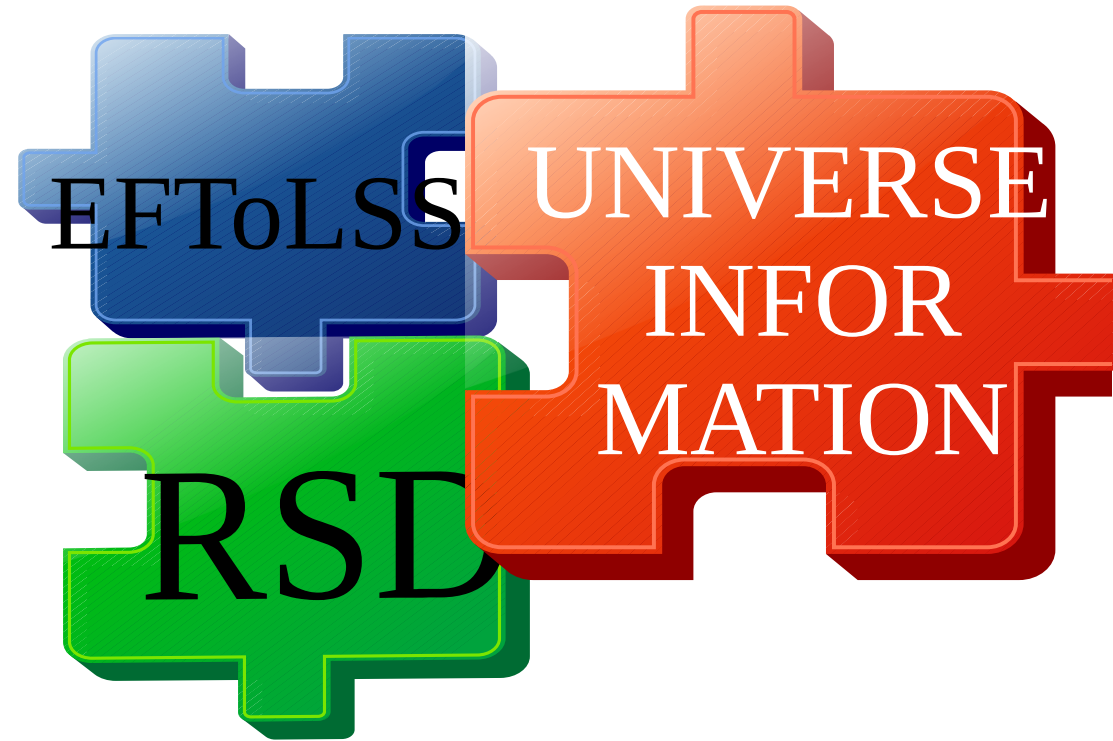
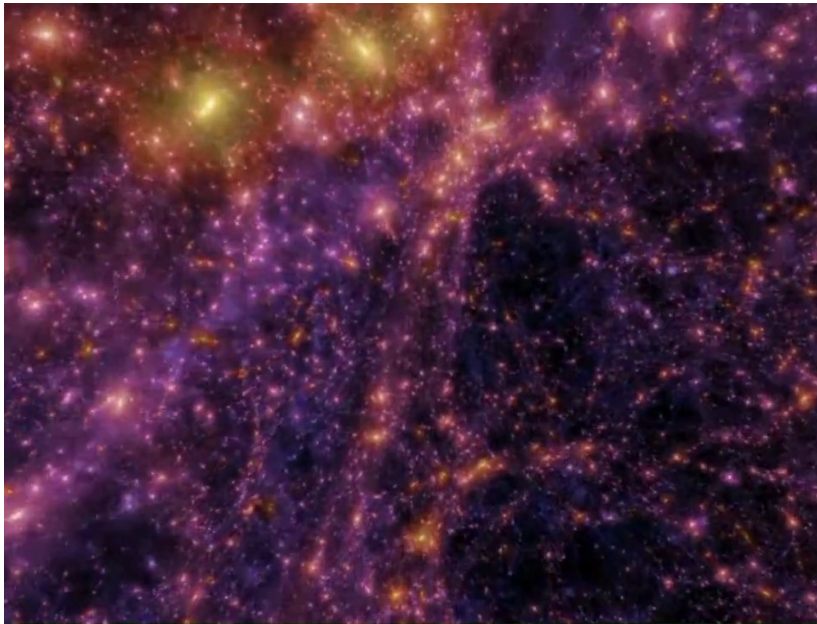
Lucía Fonseca de la Bella

University of Sussex

"...to boldly go where no one has gone before..."



...why is this important?

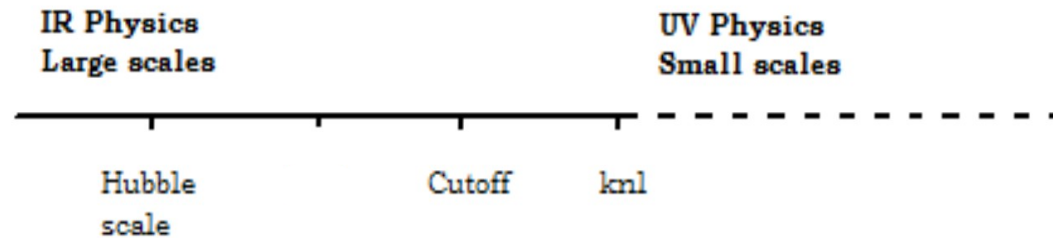


Millenium simulation, Springer et al 2005

...we'll talk about

EFToLSS- Effective Field Theory of Large Scale Structures

Carrasco, Hertzberg, Senatore 2012



- **Large Scale Structures**

- Most relevant information.
- described by the density contrast of dark matter and the matter power spectrum, P .
- Evolve almost linearly \rightarrow **PERTURBATION THEORY**

$$\delta = \frac{\Delta\rho}{\rho_0}$$

Standard Perturbation

- No good agreement with new generation of high precision observational data
- Perfect fluid
- UV divergences → Unphysical predictions

EFToLSS

- Much better fit with observations.
- Viscosity, dissipation...
- UV divergences absorbed by counterterms!

• Fluid equations in k space

$$\dot{\delta}_k + \Theta_k = - \int \frac{d^3\vec{q}d^3\vec{r}}{(2\pi)^6} (2\pi)^3 \delta(\vec{k} - \vec{q} - \vec{r}) \alpha(\vec{q}, \vec{r}) \Theta(\vec{q}) \delta(\vec{r})$$

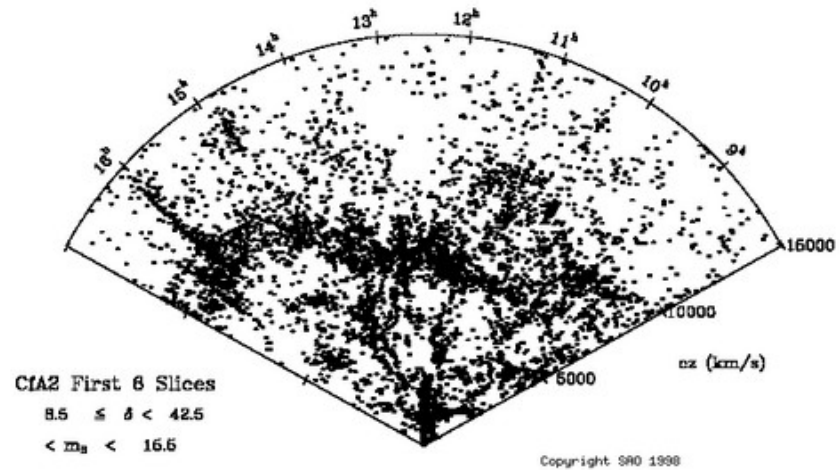
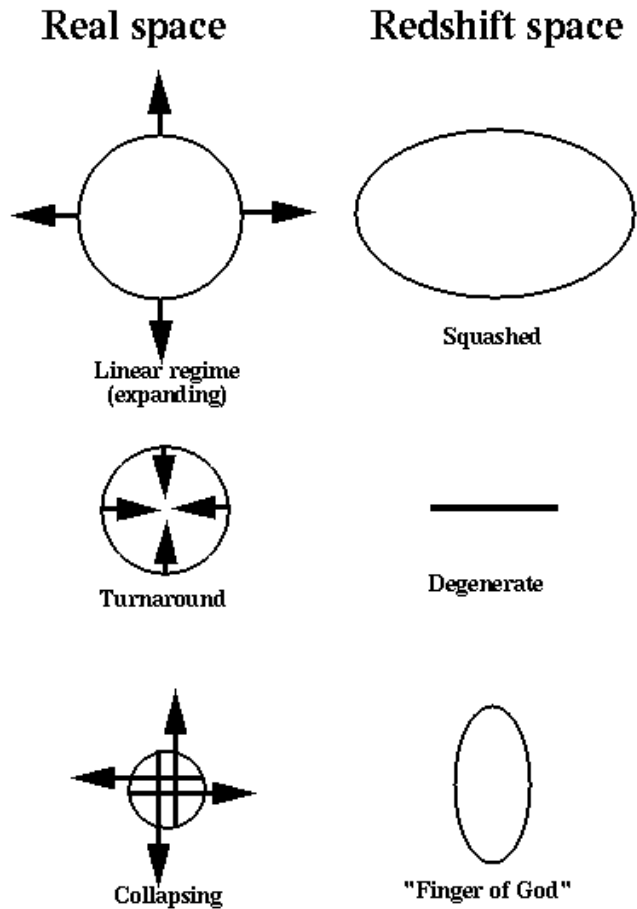
$$\dot{\Theta}_k + 2H\Theta_k + \frac{3}{2}H^2\Omega_M(z)\delta_k = \boxed{-\frac{k^2}{a^2}[Z_\delta\delta_k + Z_\Theta\Theta_k]} - \int \frac{d^3\vec{q}d^3\vec{r}}{(2\pi)^6} (2\pi)^3 \delta(\vec{k} - \vec{q} - \vec{r}) \beta(\vec{q}, \vec{r}) \Theta(\vec{q}) \Theta(\vec{r})$$

Theta is the divergence of the velocity field, alpha and beta are kernels.

RSD- *Redshift Space Distortions*



Kaiser 1987

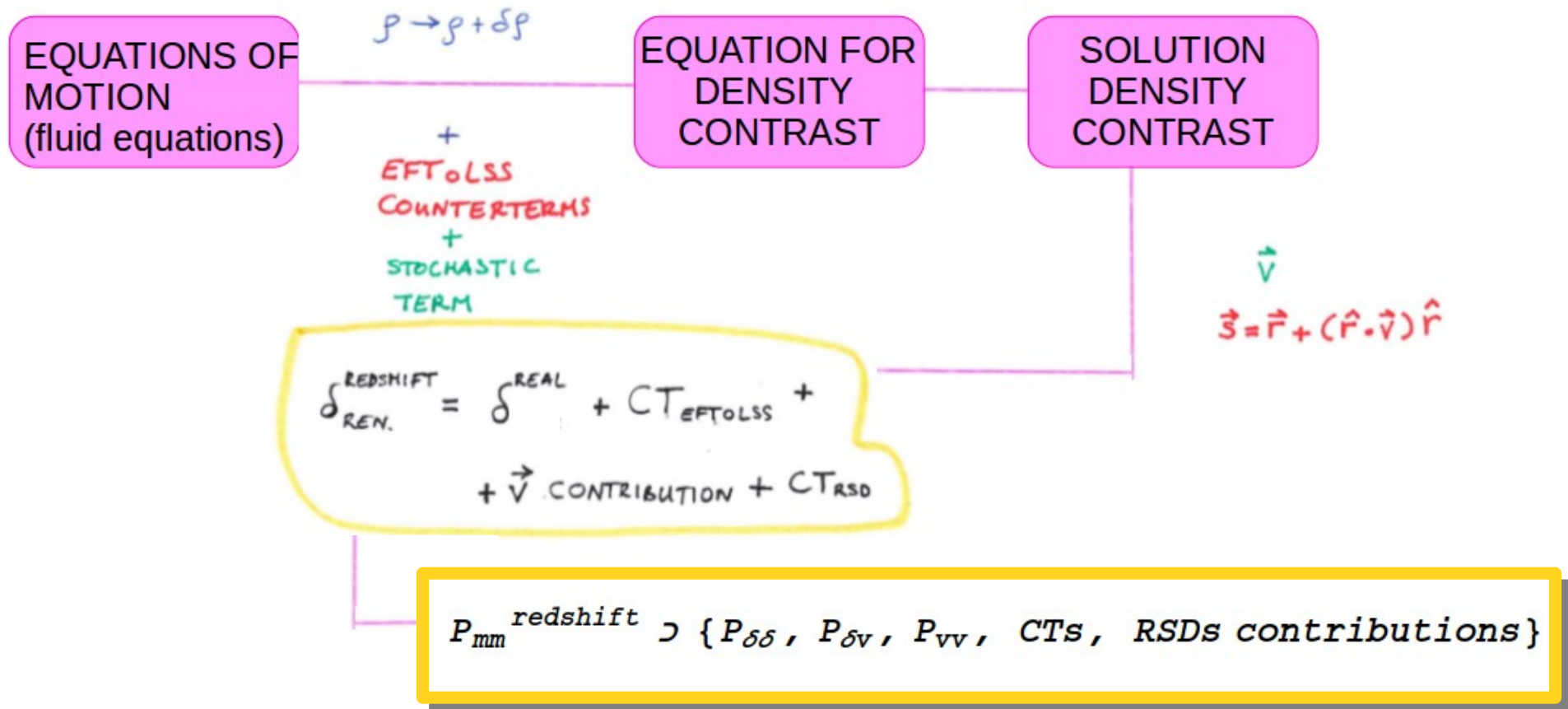


- Learn about velocities.
- Additional counterterm (CT) contributions to the matter power spectrum involving **velocity fields**.

EFToLSS & RSD

Senatore, Zaldarriaga 2014

- Power spectrum $\langle \delta^*(k, z)\delta(k', z) \rangle = (2\pi)^3 \delta_D(\vec{k} + \vec{k}') P(k, z)$



...1-loop matter power spectrum in Redshift Space

$$\begin{aligned}
 P_{r,\delta,\delta, ||1\text{-loop}}(k, \mu, t) = & P_{\delta,\delta, ||1\text{-loop}}(k, t) + 2\mu^2 P_{\delta, \frac{\delta}{H}, ||1\text{-loop}}(k, t) \\
 & + \mu^4 P_{\frac{\delta}{H}, \frac{\delta}{H}, ||1\text{-loop}}(k, t) - \left(\frac{k\mu}{aH}\right)^2 P_{\delta, [v_z^2], \text{tree}}(k, t) \\
 & - \mu^2 \left(\frac{k\mu}{aH}\right)^2 P_{\frac{\delta}{H}, [v_z^2], \text{tree}}(k, t) + \frac{1}{4} \left(\frac{k\mu}{aH}\right)^4 P_{[v_z^2], [v_z^2], \text{tree}}(k, t) \\
 & + (1 + f\mu^2) \left(\frac{k\mu}{aH}\right)^2 P_{\delta, [\delta v_z^2], \text{tree}}(k, t) + \frac{i}{3} (1 + f\mu^2) \left(\frac{k\mu}{aH}\right)^2 P_{\delta, [v_z^3], \text{tree}}(k, t) \\
 & - (1 + f\mu^2) [(c_1 + c_2) \mu^2 + (c_1 + c_3) \mu^4] \left(\frac{k}{k_{\text{NL}}}\right)^2 P_{\delta, \delta, 11}(k, t) ,
 \end{aligned}$$

UV DIVERGENCES AND RENORMALISATION

	LOCAL	NON-LOCAL	EFFECTS
MANIFEST BY	ANALYTIC	NON-ANALYTIC	TERMS
STRUCTURE	=	≠	COUNTERTERMS
CUTOFF	DEPENDENT	INDEPENDENT	
PHYSICAL	X	✓	
PREDICTED BY EFFECTIVE THEORY	X	✓	

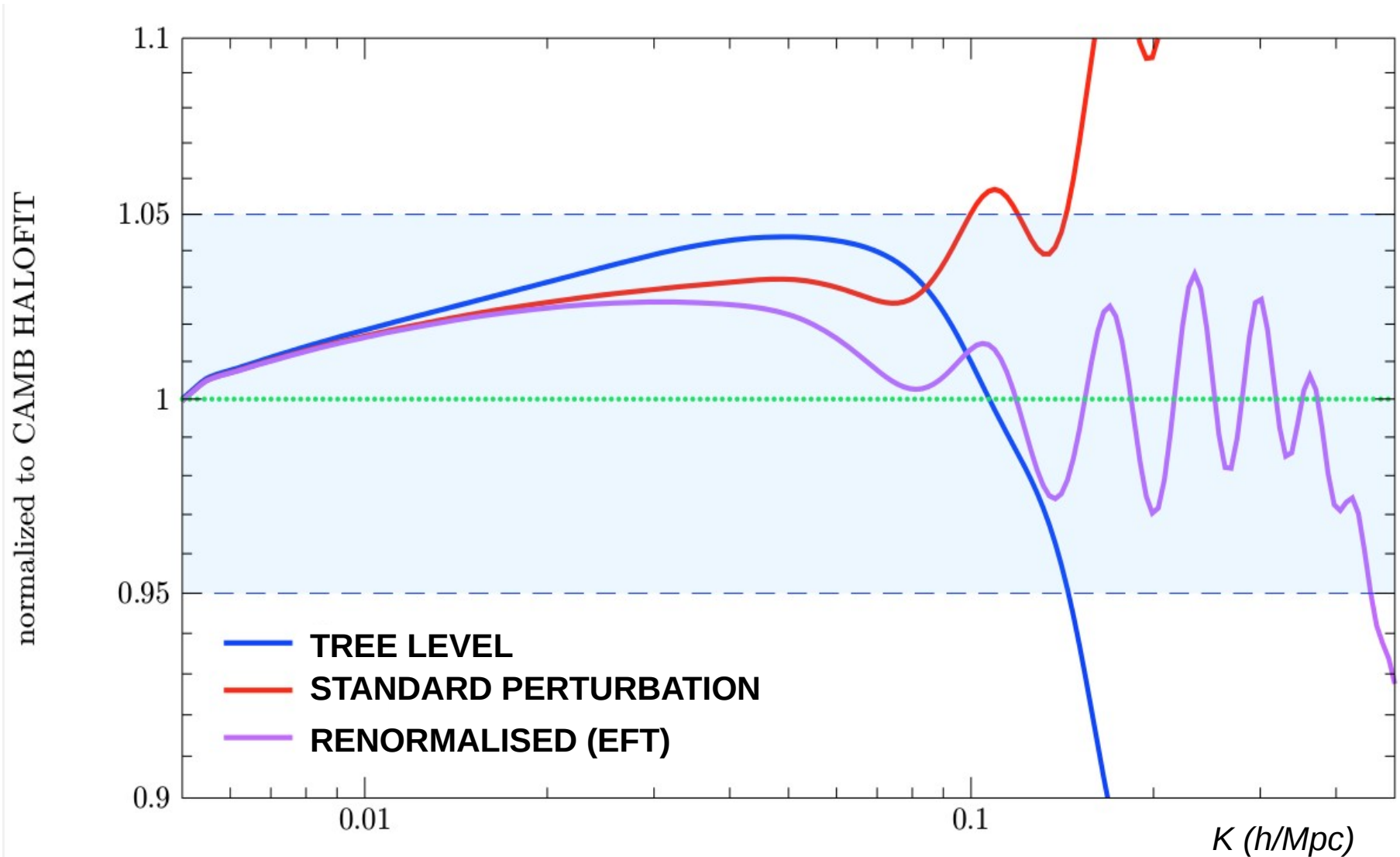
- Local in wave number, k .
- Analytic means polynomial in k^2 .
- Non-analytic, log or fractional powers of k^2 .

- Example of loop integrals in momentum space found in P_{13}

$$\begin{aligned}
 I_{\alpha\alpha}(\Lambda) &= \int^{\Lambda} \frac{d^3\vec{q}}{(2\pi)^3} \mathcal{P}_R(\vec{q}) \alpha(\vec{k}, -\vec{q}) \alpha(\vec{k} - \vec{q}, \vec{q}) \\
 &= \underbrace{\int_0^{k_*} \frac{d^3\vec{q}}{(2\pi)^3} \mathcal{P}_R(\vec{q}) \alpha(\vec{k}, -\vec{q}) \alpha(\vec{k} - \vec{q}, \vec{q})}_{k_* \ll k \text{ regime, } \Lambda\text{-independent}} + \underbrace{\int_{k_*}^{\Lambda} \frac{d^3\vec{q}}{(2\pi)^3} \mathcal{P}_R(\vec{q}) \alpha(\vec{k}, -\vec{q}) \alpha(\vec{k} - \vec{q}, \vec{q})}_{k/k_* \ll 1 \text{ Taylor expansion, } \Lambda\text{-dependent}} \\
 &= \underbrace{a_1(\Lambda)}_{\substack{\text{fixed by renormalisation} \\ \text{analytic behaviour, UV sensitive}}} \cdot k^2 + \underbrace{b_1}_{\substack{\text{low-energy} \\ \text{Non-analytic}}} \cdot k^3 + O(k^4).
 \end{aligned}$$


COUNTERTERMS
Fit cubic polynomial

1 LOOP MATTER POWER SPECTRUM



Repeat analysis for $P_{\delta, \frac{\delta}{H}, ||_{1\text{-loop}}}(k, t)$, $P_{\frac{\delta}{H}, \frac{\delta}{H}, ||_{1\text{-loop}}}(k, t)$ and rest of counterterms



CONCLUSIONS

- The Universe is treated as a fluid. Most of the relevant information in Cosmology is found at **large scales**.
- At large scales, galaxies are point-like objects. There exist voids, filaments, clusters of galaxies...
- We want to study the **backreaction** from small scales and the so-called **Redshift Space Distortion** effect on large scale structures.
- Simulations are very expensive. We would need to run several simulations with different initial conditions.
- **Effective Field Theory of Large Scale Structures** is a powerful tool
 - This framework solves those theoretical **issues** present in **Standard perturbation** theory.
 - Some parameters need to be included in the analytical prediction and need to be measured by matching to numerical data → **Renormalisation**.
 - It agrees much better with new high precision observational datasets.

& PROSPECTS

- To obtain the renormalisation for the 1 loop matter power spectrum in Redshift Space.
- Compare with observations and N-body simulations.
- To apply this tool to the analysis of the **screening mechanism** in theories of **Modified Gravity**.

VILA DO CONDE,
PORTUGAL,
29-31 MARCH, 2016

11th Iberian Cosmology Meeting

IBERICOS 2016

SOC ANA ACHÚCARRO (LEIDEN/BILBAO),
FERNANDO ATRIO-BARANDELA (SALAMANCA),
MAR BASTERO-GIL (GRANADA), JUAN GARCIA-
BELLIDO (MADRID), RUTH LAZKOZ (BILBAO),
CARLOS MARTINS (PORTO), JOSÉ PEDRO
MIMOSO (LISBON), DAVID MOTA (OSLO)

LOC ANA CATARINA LEITE, CARLOS MARTINS
(CHAIR), FERNANDO MOUCHEREK, PAULO
PEIXOTO (SYSADMIN), ANA MARTA PINHO,
IVAN RYBAK, ELSA SILVA (ADMIN)

SERIES OF MEETINGS WHICH AIM
TO ENCOURAGE INTERACTIONS
AND COLLABORATIONS BETWEEN
RESEARCHERS WORKING IN
COSMOLOGY AND RELATED
AREAS IN PORTUGAL AND SPAIN.

www.iastro.pt/ibericos2016





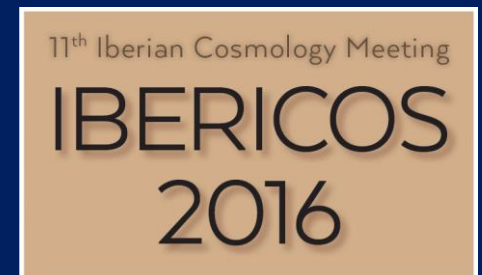
X-ray L-T relation for the XMM Cluster Survey by parameteric and non-parametric Bayesian Statistics

Leyla S. Ebrahimpour

Supervisor:
Pedro T. P. Viana



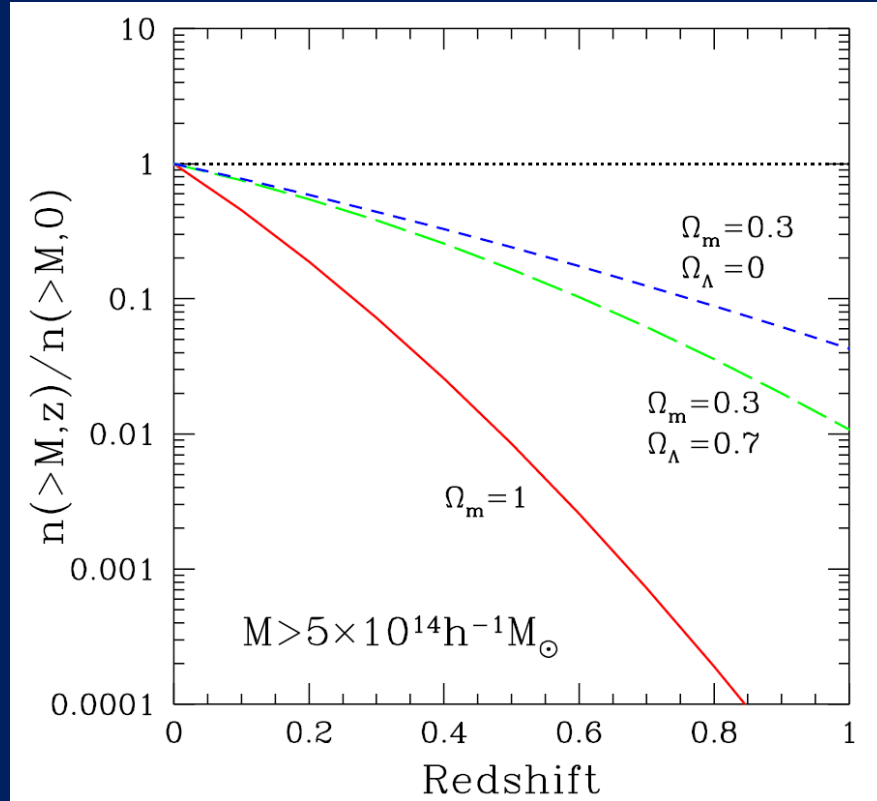
29 March 2016



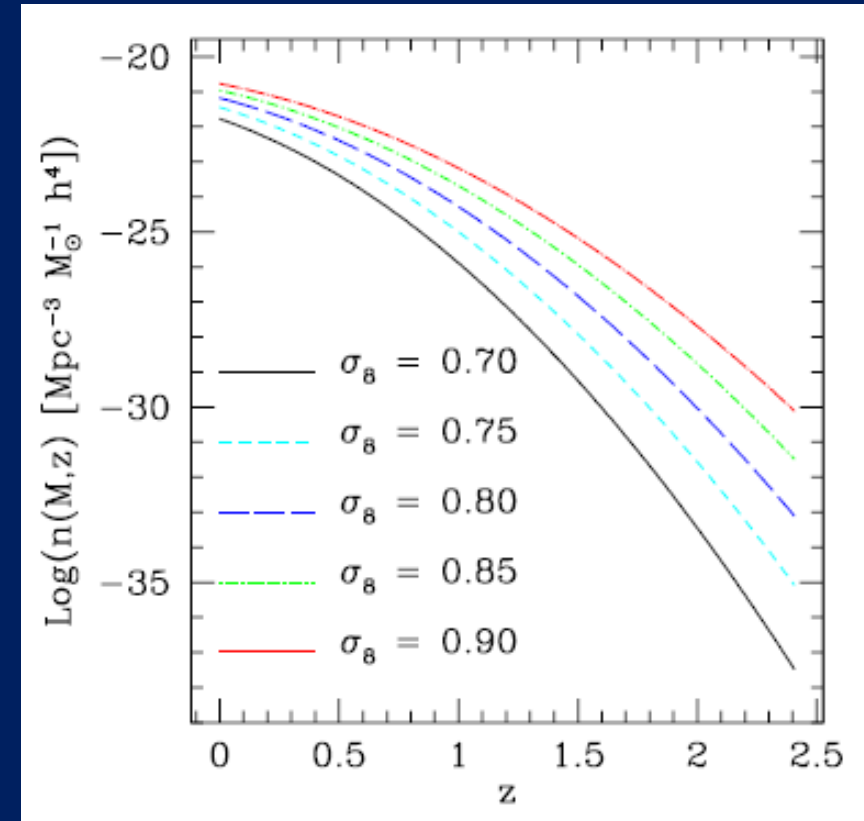
Introduction

Properties of galaxy clusters:

- Characterize the growth of structure in the Universe
- Constrain the cosmological parameters



S. Borgani, 2003



Fedeli et al, A&A, 486, 2008

Introduction

Precise knowledge of mass  Direct methods
Indirect methods: Scaling Relations

Scaling Relations

- Relate the fundamental properties of galaxy clusters
- Carry information about the thermodynamical history of the intra-cluster medium, and the non-gravitational processes that have taken place

Introduction

XMM Cluster Survey (XCS)

- X-ray galaxy cluster survey
- 346 optically confirmed galaxy clusters
- $0.06 < z < 1.39$
- $0.44 \text{ KeV} < \text{Temperature} < 9.89 \text{ KeV}$
- $4.36 \times 10^{41} \text{ erg/s} < \text{Luminosity} < 3.84 \times 10^{45} \text{ erg/s}$

Work done

Statistical Framework : Parametric Bayesian Statistics

$$\mathbf{Y} = \alpha + \beta\mathbf{X} + \gamma\mathbf{T} + \epsilon$$

$$y_i \sim N(Y_i, \delta_{y,i})$$

$$x_i \sim N(X_i, \delta_{x,i})$$

$$\theta \equiv (\alpha, \beta, \gamma, \epsilon)$$



$$p(\theta|x, y) \propto p(x, y|\theta)p(\theta)$$

Posterior

likelihood

Prior

$$\log(L/E_z) = \alpha + \beta \log(T/5) + \gamma \log(1+z) + \epsilon$$

$$E_z = (0.27 \times (1+z)^3 + 0.73)^{1/2}$$

Work done

R programming :lira

Mauro Sereno, <http://arxiv.org/pdf/1509.05778v2.pdf>

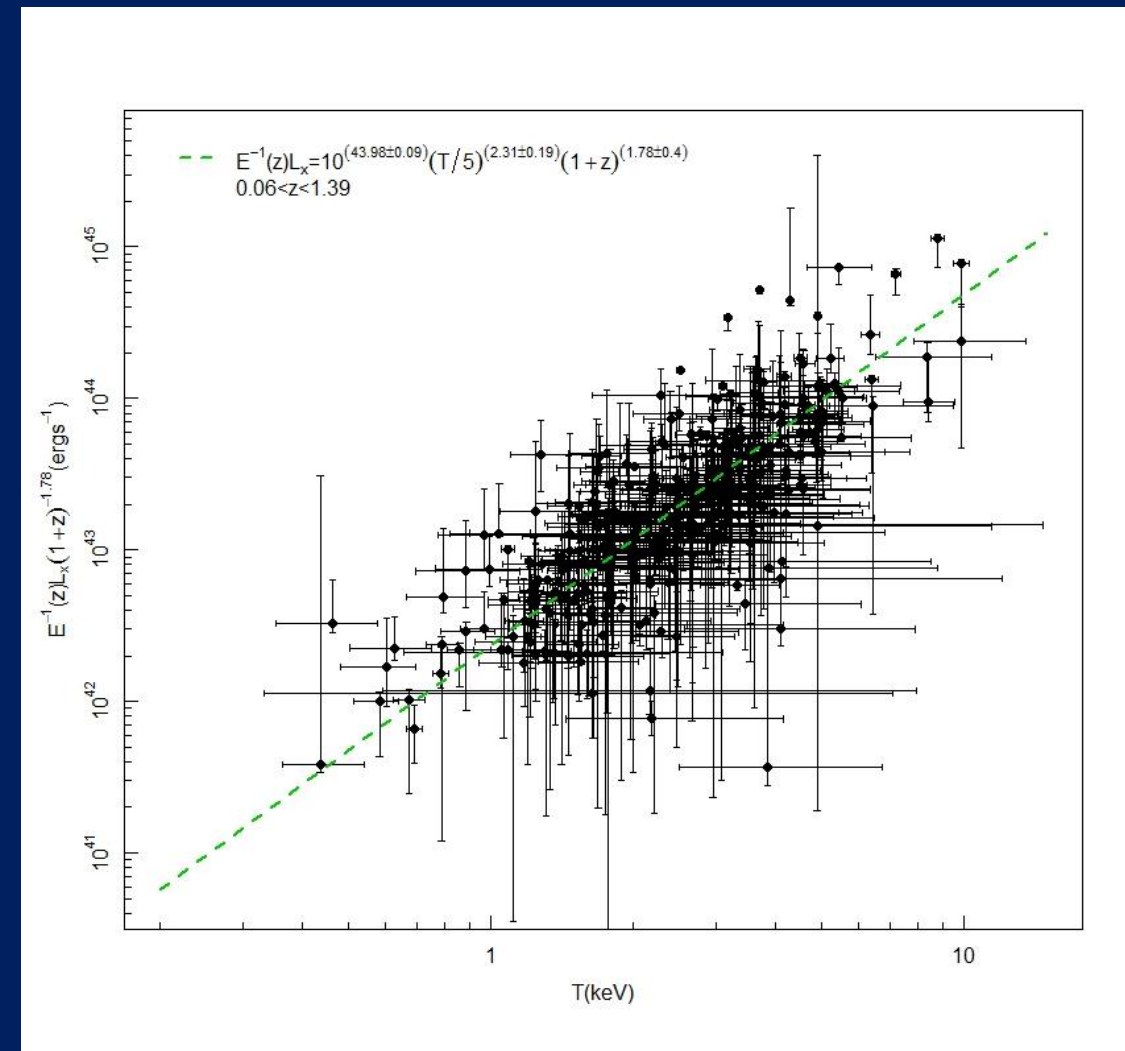
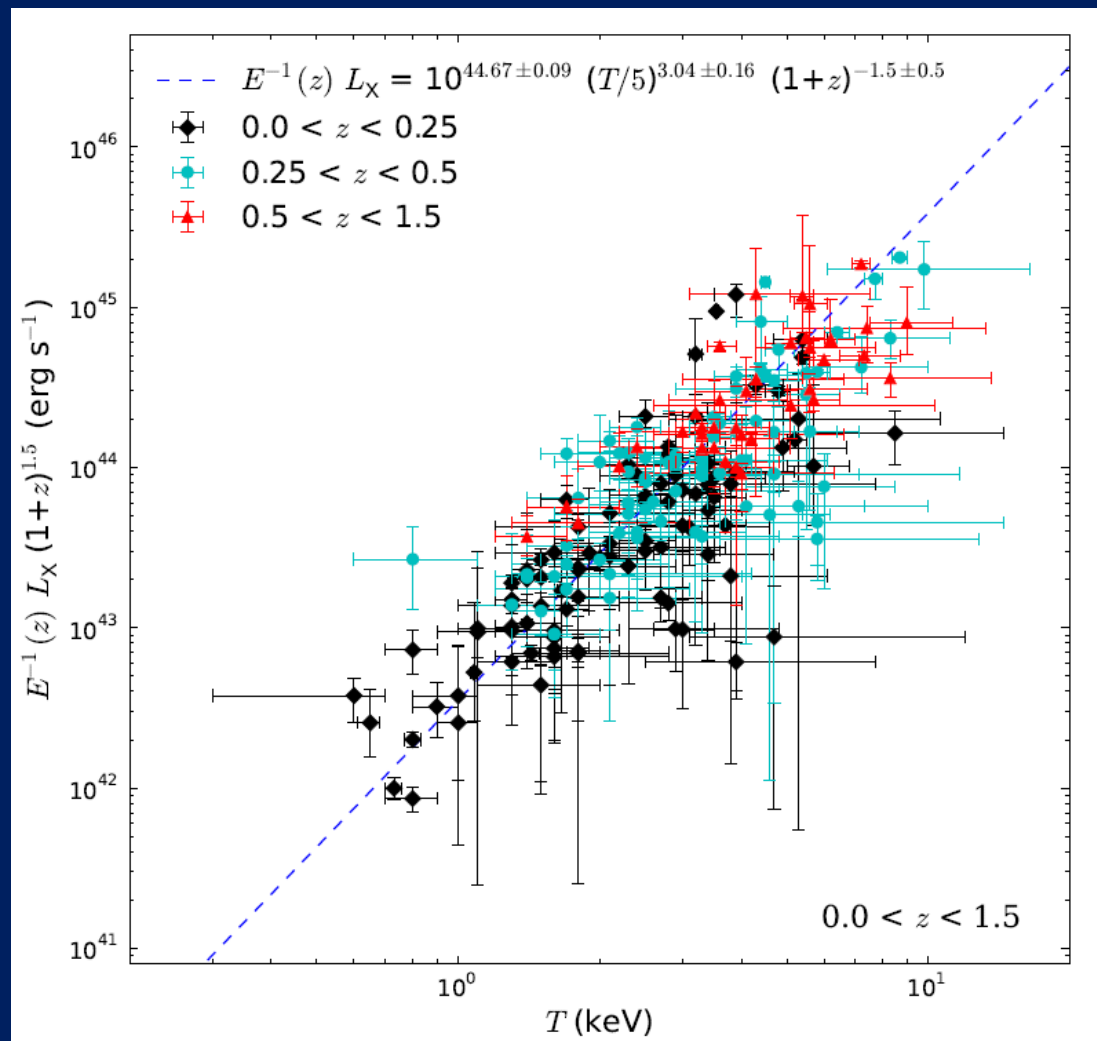
- No selection function
- Flux cut as a simple selection function

Priors for Temperature ($\log(T)$):

- ✓ Uniform
- ✓ Gaussian
- ✓ Truncated Gaussian (Considering clusters with $T > 2$ KeV)

Work done

L-T scaling relation



Work done

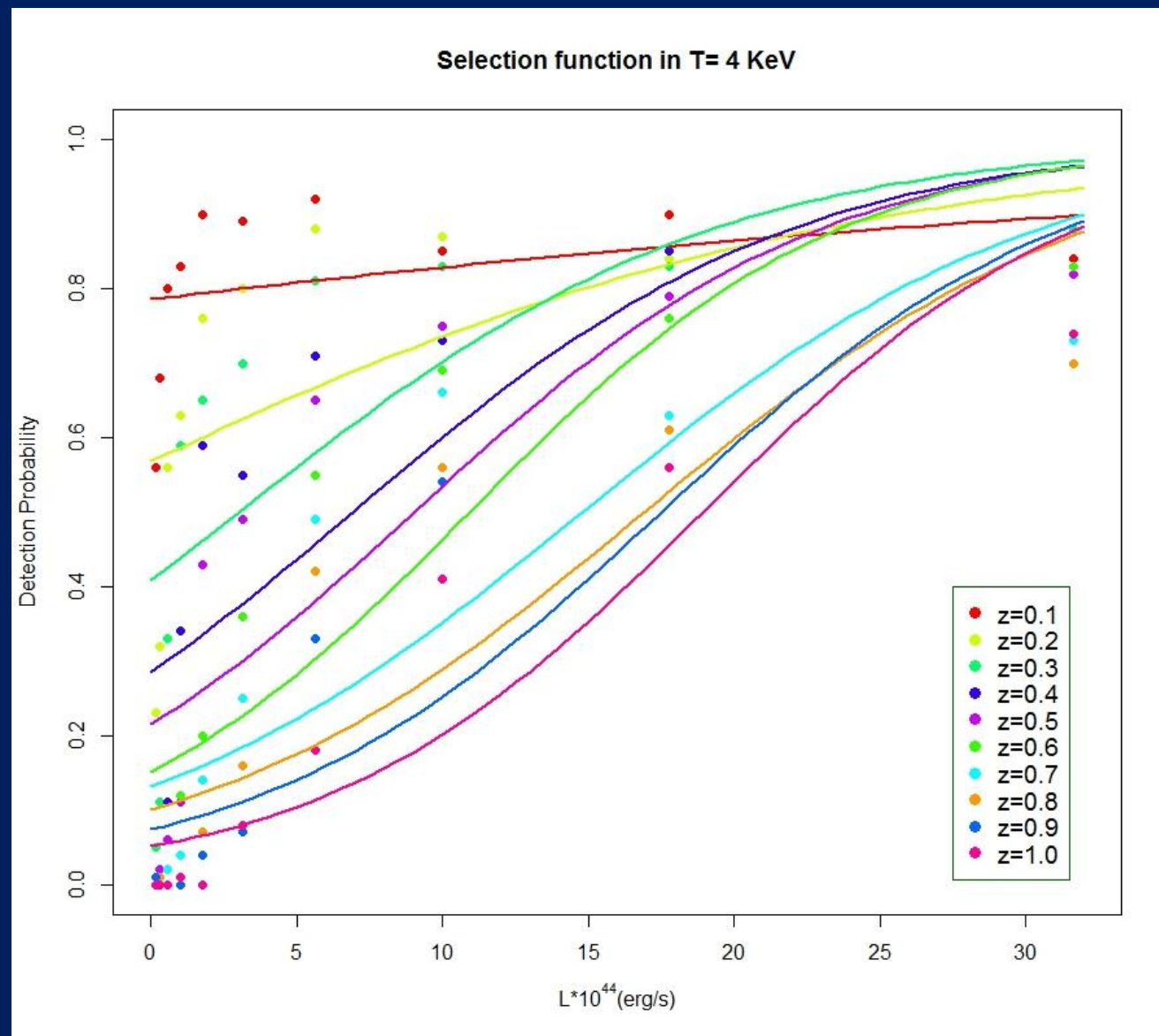
XCS Selection function

Fitted to a logistic function by
Bayesian statistics

Cauchy distributions are recommended
on all logistic regression coefficients as
the priors *Gelman et al., AAS, Vol. 2, 2008*

R programming: bayesglm

$$p = 1 / (1 + \exp \left(- \left((1.2 \pm 0.31) - (3.91 \pm 0.38)z + (0.13 \pm 0.01)L - (0.09 \pm 0.05)T \right) \right))$$



Work done

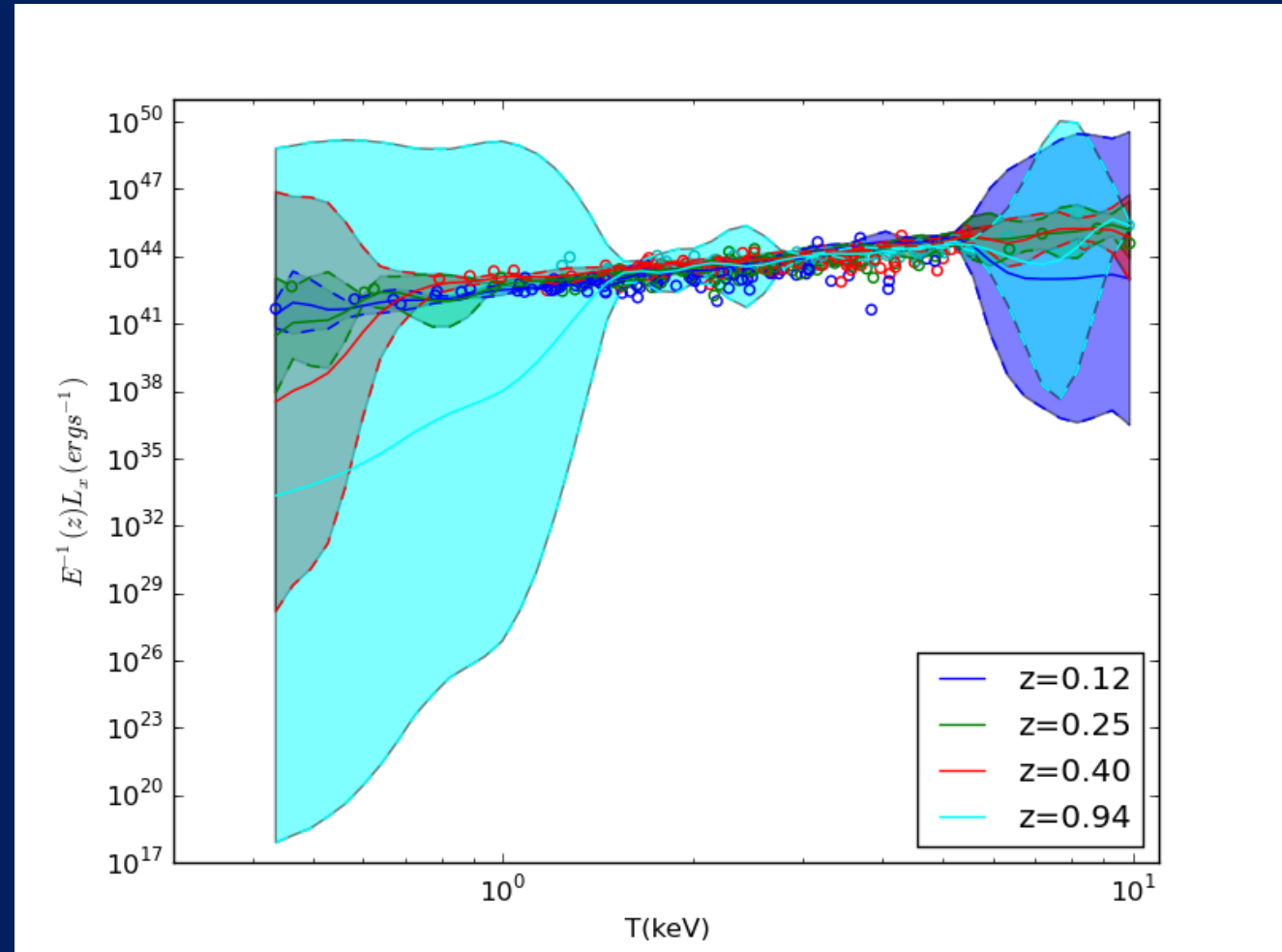
Statistical Framework : Non-Parametric Bayesian Statistics

- Gaussian Processes

Python Programming: GaPP

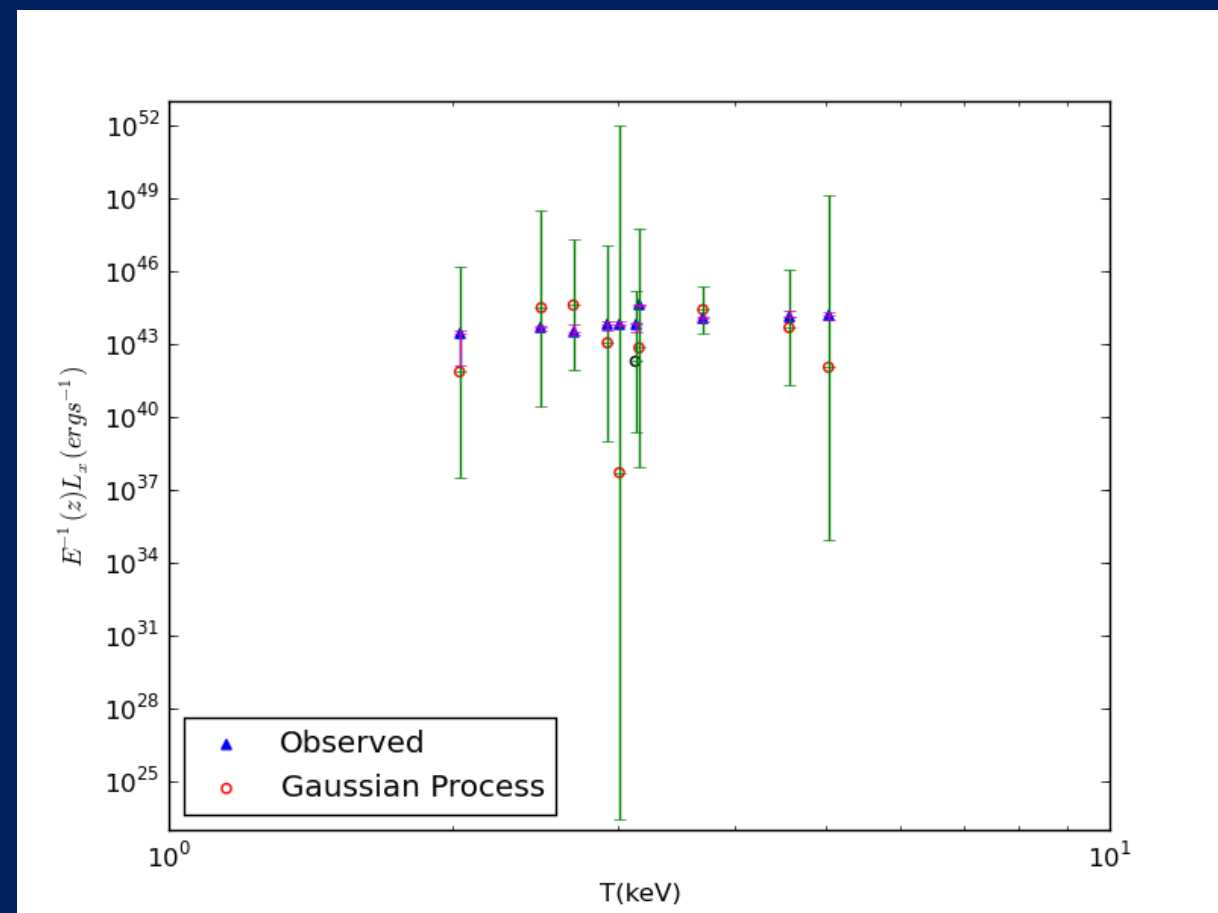
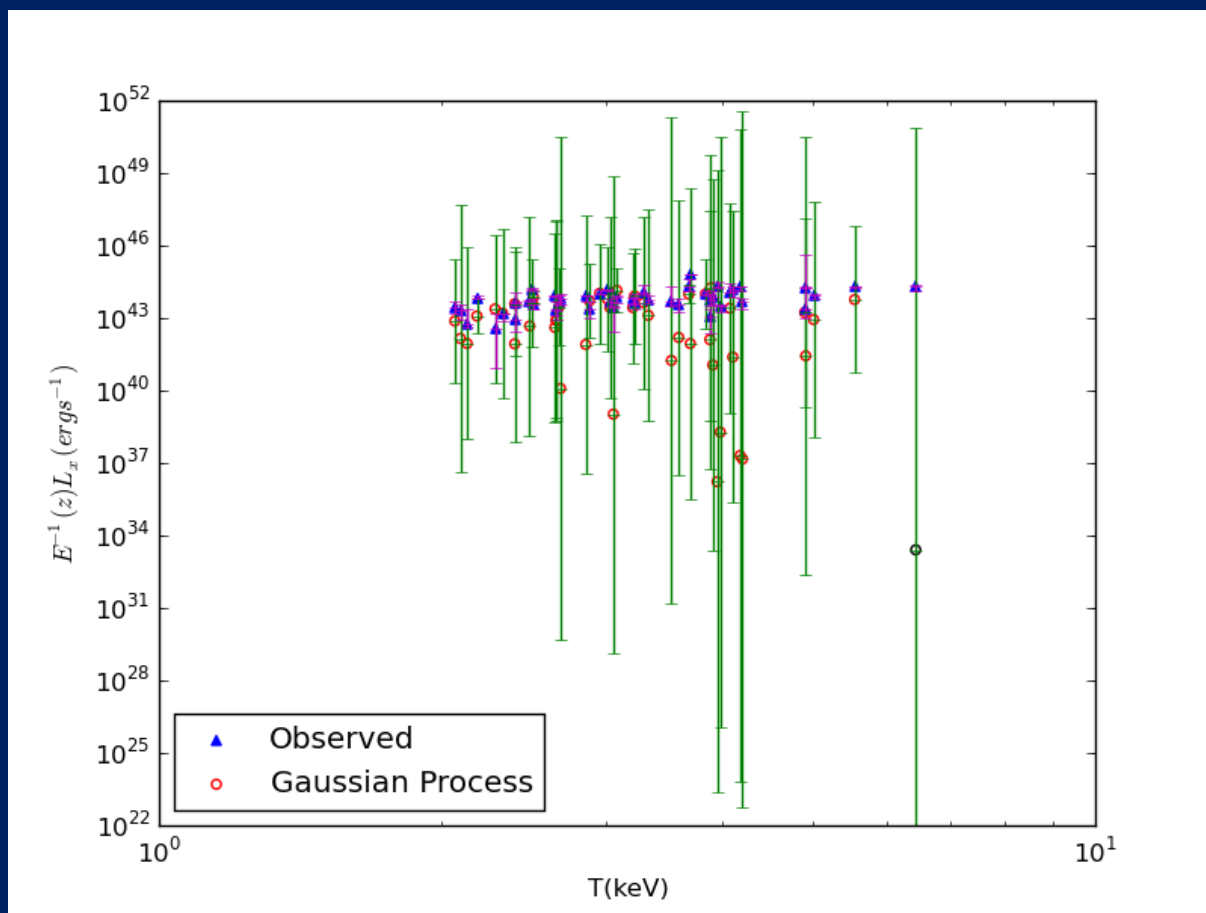
M. Seikel et al., JCAP, 2012

- Temperature and redshift as predictors
- Marginalize over hyperparameters of covariance function



Work done

Luminosity vs Temperature by Non-Parametric results



Ongoing and Future work

- Apply the selection function by Parametric and Non-Parametric schemes
- Apply the methods on other galaxy clusters data in different wavelengths
- Use the methods to construct the mass of clusters based on galaxy clusters properties in different wavelengths

Thanks for your attention

VILA DO CONDE,
PORTUGAL,
29-31 MARCH, 2016

11th Iberian Cosmology Meeting

IBERICOS 2016

SOC ANA ACHÚCARRO (LEIDEN/BILBAO),
FERNANDO ATRIO-BARANDELA (SALAMANCA),
MAR BASTERO-GIL (GRANADA), JUAN GARCIA-
BELLIDO (MADRID), RUTH LAZKOZ (BILBAO),
CARLOS MARTINS (PORTO), JOSÉ PEDRO
MIMOSO (LISBON), DAVID MOTA (OSLO)

LOC ANA CATARINA LEITE, CARLOS MARTINS
(CHAIR), FERNANDO MOUCHEREK, PAULO
PEIXOTO (SYSADMIN), ANA MARTA PINHO,
IVAN RYBAK, ELSA SILVA (ADMIN)

SERIES OF MEETINGS WHICH AIM
TO ENCOURAGE INTERACTIONS
AND COLLABORATIONS BETWEEN
RESEARCHERS WORKING IN
COSMOLOGY AND RELATED
AREAS IN PORTUGAL AND SPAIN.

www.iastro.pt/ibericos2016



The CMB temperature-redshift relation as tool to probe the standard cosmology

Ivan de Martino

IberiCOS 2016, March 29th, 2016

in collaboration with F. Atrio-Barandela, C.J.A.P. Martins, et al.

From T_{CMB} to $\frac{\Delta\alpha}{\alpha}$

Adiabatic evolution

$$T_{CMB}(z) = T_0(1+z)$$

No adiabatic evolution

$$\frac{T_{CMB}(z)}{T_0} \sim (1+z) \left(1 + \epsilon \frac{\Delta\alpha}{\alpha}\right), \quad [\text{Avgoustidis, et al. JCAP 06 62(2014)}].$$

Observations of dipole spatial variation of $\frac{\Delta\alpha}{\alpha}$

- spectroscopic measurements of quasars $\Delta\alpha/\alpha = (0.61 \pm 0.20) \times 10^{-5}$ [Webb, J.K. et al. *Phys. Rev. Lett.* 107 191101 (2011)];
- CMB power spectrum $\Delta\alpha/\alpha = (-2.4 \pm 3.7) \times 10^{-2}$ [Planck Collaboration, *A&A* 580 A22 (2015)];
- SZ/X-ray scaling relation $\Delta\alpha/\alpha = (-5.5 \pm 7.9) \times 10^{-3} \text{GLyr}^{-1}$ [Galli, S., *Phys. Rev. D* 87, 123516 (2013)].

From the SZ effect to T_{CMB}

Temperature anisotropies due to SZ effects are given by

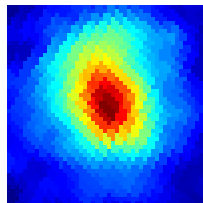
$$\frac{\Delta T}{T} = g(\nu) Y_c(\theta),$$

and their frequency dependence by

$$x = \frac{h\nu(z)}{k_B T_{CMB}(z)} \quad g(\nu) = x \coth(x) - 4.$$

If we treat the CMB temperature at cluster location as a free parameter to constraint then

$$g(\nu) \mapsto g(\nu, T_{CMB}(z))$$



Recipe and ingredients

Ingredients

- X-ray cluster catalog with well measured positions and redshifts
- *Planck* 2013 Nominal maps

Recipe

STEP 1: you should clean *Planck* 2013 Nominal maps from foreground emission (i.e. thermal dust, CO lines, synchrotron and etc...)

STEP 2: you may measure the TSZ emission at cluster location and extract the CMB temperature

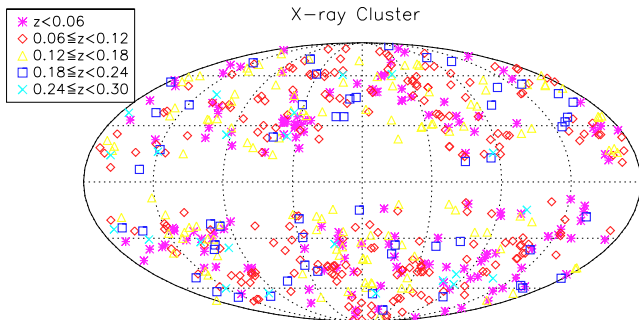
STEP 3: Once you have done, everything is ready to carry out tests of the spatial variation of the fine structure constant

X-ray Cluster Catalog

Our cluster sample contains almost 618 clusters outside galactic plane.

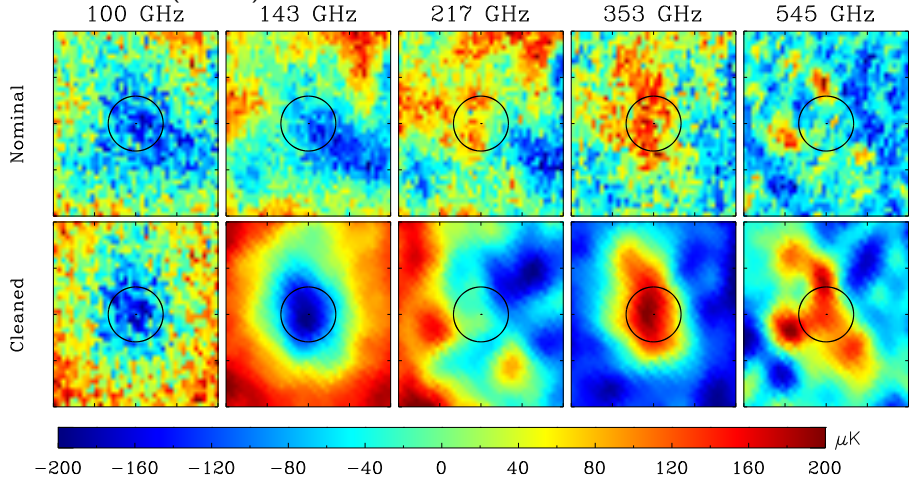
- ROSAT-ESO Flux Limited X-ray catalog (REFLEX)
- extended Brightest Cluster Sample (eBCS)
- Clusters in the Zone of Avoidance (CIZA)

All three surveys are X-ray selected and X-ray flux limited. The position, flux, X-ray luminosity, angular extent, and redshifts are measured. The X-ray temperature was derived from the $L_X - T_X$ relation [Kocevski, D. and Ebeling, H. (2006). *ApJ*, 645:1043]



Cleaning procedure: $\mathcal{P}(\nu, \mathbf{x}) = P(\nu, \mathbf{x}) - w(\nu)P(857\text{GHz}, \mathbf{x})$

Coma Cluster (A1656): $l = 57.8^\circ$; $b = 88.0^\circ$; $z = 0.02310$



[de Martino, I. et al. 2015, ApJ, 808, 128]

Obtaining T_{CMB} from the data

For each channel, we measure the TSZ emission over disc of radius θ_{500} : $\delta\bar{T}/T_0$. Then, we predict the theoretical averaged TSZ anisotropies at the same apertures

$$\Delta\bar{T}(\mathbf{p}, \nu_i)/T_0 = G(\nu_i, T_{CMB}(z))\langle Y_c \rangle_{\theta_{500}},$$

where

$$\mathbf{p} = [T_{CMB}(z), \langle Y_c \rangle_{\theta_{500}}].$$

We explore the 2D parameter space with Monte Carlo Markov Chain (MCMC) technique. We run four independent chains employing the Metropolis-Hastings sampling algorithm with different (randomly set) starting points. The chains stop when contain at least 30,000 steps and satisfy the Gelman-Rubin criteria.

Estimating $\frac{\Delta\alpha}{\alpha}$ from the data

Once we have extracted the $T_{CMB}(z)$ from the data, we are ready to estimate the variation of the fine structure constant at cluster location:

$$\left(\frac{\Delta\alpha}{\alpha}\right)_{obs} = \epsilon^{-1} \left(1 - \frac{T_{CMB}(z)}{T_0(1+z)}\right),$$

and to compare it with

Model 1. $\left(\frac{\Delta\alpha}{\alpha}\right)_{th} = m + d \cos(\Theta),$

Model 2. $\left(\frac{\Delta\alpha}{\alpha}\right)_{th} = m + dr(z) \cos(\Theta),$

where m and d are the monopole and dipole amplitudes, Θ is the angle on the sky between the line of sight of each cluster and the best fit dipole direction, and $r(z)$ is the look-back time in the concordance Λ CDM model.

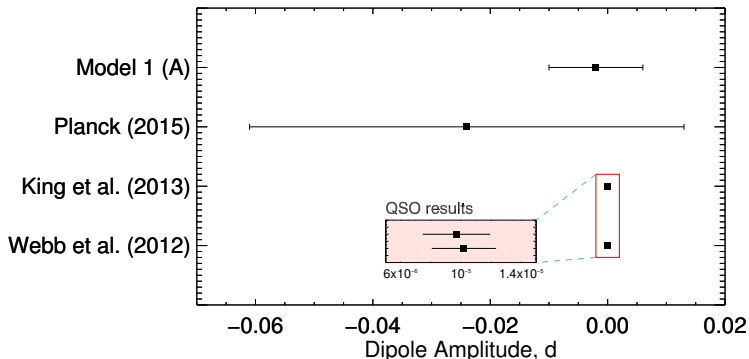
Testing $\frac{\Delta\alpha}{\alpha}$ from the data

For each model we carry out 4 different MCMC analysis: (A) we assume the monopole amplitude to be zero and the direction of the dipole to be the best fit ones from QSO. The model has one free parameter (i.e. the dipole amplitude). (B) we still keep the direction of the dipole fixed at the best fit ones from QSO, but we leave the monopole and dipole amplitudes free to vary. In (C) and (D) we repeat the analysis as they are in (A) and (B) leaving the direction of the dipole free to vary.

Analysis	m	d	RA ($^{\circ}$)	DEC ($^{\circ}$)	N_{par}
(A)	0	$[-1, 1]$	261.0	-58.0	1
(B)	$[-1, 1]$	$[-1, 1]$	261.0	-58.0	2
(C)	0	$[-1, 1]$	$[0, 360]$	$[-90, +90]$	3
(D)	$[-1, 1]$	$[-1, 1]$	$[0, 360]$	$[-90, +90]$	4

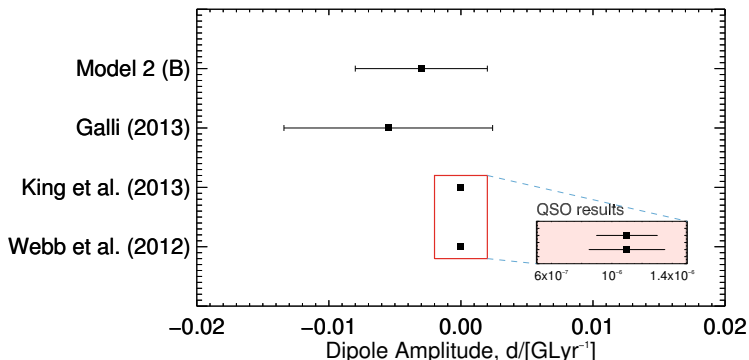
Results from Model 1

Analysis	m	d	RA ($^{\circ}$)	DEC ($^{\circ}$)
(A)	0	-0.002 ± 0.008	261.0	-58.0
(B)	0.006 ± 0.04	-0.008 ± 0.009	261.0	-58.0
(C)	0	-0.030 ± 0.020	255.1 ± 3.8	-63.2 ± 2.6
(D)	0.02 ± 0.03	-0.030 ± 0.014	255.9 ± 4.2	55.3 ± 5.8



Results from Model 2

Analysis	m (GLyr^{-1})	d (GLyr^{-1})	RA ($^\circ$)	DEC ($^\circ$)
(A)	0	-0.003 ± 0.003	261.0	-58.0
(B)	0.006 ± 0.0045	-0.003 ± 0.005	261.0	-58.0
(C)	0	-0.004 ± 0.005	261.6 ± 16.1	-61.3 ± 2.7
(D)	0.02 ± 0.01	-0.003 ± 0.005	245.0 ± 12.9	-56.0 ± 3.8



Conclusions

We have constrained the spatial variation of the fine structure constant using Planck data.

1. Cluster are not competitive with QSO **but** they play an equally important role since allow to probe a different redshift range.
2. Introducing the dependence from the look-back time in Model 2 does not help to improve the final results that are still compatible with zero. *This was expected since our dataset is at $z < 0.3$.*
3. Our best constraints are obtained when the dipole direction is fixed to the best fit ones from QSO.
4. Our results improve previous analysis of Planck Collaboration and other groups.

VILA DO CONDE,
PORTUGAL,
29-31 MARCH, 2016

11th Iberian Cosmology Meeting

IBERICOS 2016

SOC ANA ACHÚCARRO (LEIDEN/BILBAO),
FERNANDO ATRIO-BARANDELA (SALAMANCA),
MAR BASTERO-GIL (GRANADA), JUAN GARCIA-
BELLIDO (MADRID), RUTH LAZKOZ (BILBAO),
CARLOS MARTINS (PORTO), JOSÉ PEDRO
MIMOSO (LISBON), DAVID MOTA (OSLO)

LOC ANA CATARINA LEITE, CARLOS MARTINS
(CHAIR), FERNANDO MOUCHEREK, PAULO
PEIXOTO (SYSADMIN), ANA MARTA PINHO,
IVAN RYBAK, ELSA SILVA (ADMIN)

SERIES OF MEETINGS WHICH AIM
TO ENCOURAGE INTERACTIONS
AND COLLABORATIONS BETWEEN
RESEARCHERS WORKING IN
COSMOLOGY AND RELATED
AREAS IN PORTUGAL AND SPAIN.

www.iastro.pt/ibericos2016

